



Dynamical analysis of a glucose-insulin regulatory system with insulin-degrading enzyme and multiple delays

Feng Rao¹ · Zhongliang Zhang¹ · Jiaxu Li²

Received: 2 October 2021 / Revised: 28 December 2022 / Accepted: 18 September 2023 /
Published online: 19 October 2023

© The Author(s), under exclusive licence to Springer-Verlag GmbH Germany, part of Springer Nature 2023

Abstract

This paper investigates the dynamics of a glucose-insulin regulatory system model that incorporates: (1) insulin-degrading enzyme in the insulin equation; and (2) discrete time delays respectively in the insulin production term, hepatic glucose production term, and the insulin-degrading enzyme. We provide rigorous results of our model including the asymptotic stability of the equilibrium solution and the existence of Hopf bifurcation. We show that analytically and numerically at a certain value the time delays driven stability or instability occurs when the corresponding model has an interior equilibrium. Moreover, we illustrate the oscillatory regulation and insulin secretion via numerical simulations, which show that the model dynamics exhibit physiological observations and more information by allowing parameters to vary. Our results may provide useful biological insights into diabetes for the glucose-insulin regulatory system model.

Keywords Glucose-insulin regulatory system · Insulin degradation · Time delay · Hopf bifurcation

Mathematics Subject Classification 37N25 · 92C60 · 34K20

1 Introduction

Diabetes mellitus is a chronic disease of the glucose-insulin regulatory system, which is characterized by hyperglycemia resulting from none or little insulin release for type 1 diabetes mellitus (TDM1), or for type 2 diabetes mellitus (T2DM) due to primarily

✉ Feng Rao
raofeng2002@163.com

✉ Jiaxu Li
jjiaxu.li@louisville.edu

¹ School of Physical and Mathematical Sciences, Nanjing Tech University, Nanjing 211816, Jiangsu, China

² Department of Mathematics, University of Louisville, Louisville, KY 40292, USA

insulin resistance, a concept that the cells, e.g., muscle cells and adipose cells, are unable to utilize insulin efficiently (Chen and Tsai 2010). Diabetes mellitus can cause a variety of serious health complications including possible blindness, heart disease, kidney failure, stroke, nerve damage, and lower extremity amputations. The diabetic population in the world is rapidly rising in recent decades. International Diabetes Federation estimates that the number of subjects around the world living with diabetes is expected to hit 700 million people in 2045 (IDF 2020). It is critical to prevent the onset of diabetes or slow down its progression and thus the characteristic complications by efficient and effective interventions, for example, developing algorithms for insulin administration protocols through great understanding of the homeostasis of the glucose-insulin regulatory system.

It is well known that natural sciences and mathematical modeling have impelled each other in their progress in the long time history, well documented usefulness of mathematical models in physics and technologies, from the days of Galileo, Kepler, and Newton to present, and also in biology, for example, the Hodgkin-Huxley model of the action potentials in neurons. Particularly and naturally physiological systems are refractory to precise quantitative description by mathematical models as numerous details exist in each different level of subtle interactions (Torres and Santos 2015), which requires model refinements with the progress of deeper understandings and new findings in the related area. A footmark for the mathematical modeling approach in the study of diabetic disease can be found in 1961 by Bolie (1961). Gradually and increasingly more models are proposed to be more accurate and clinically feasible, making them a valuable resource for clinical research and applications. One example is the *Minimal Model* by Bergman et al. (1979) and many consequent works for the intravenous glucose tolerance test (IVGTT) used to assess insulin sensitivity and glucose effectiveness. Another example is a series of models proposed and refined or extended by Chen and Tsai (2010), Sturis et al. (1991), Tolic et al. (2000), Engelborghs et al. (2001), Li et al. (2006), Li and Kuang (2007) for understanding the regulating mechanisms of the glucose-insulin system including the sustained ultradian oscillations of insulin secretion. Among which, as commented by Batzel and Kappel (2011), the delay differential equation model refined by Li et al. (2006), Li and Kuang (2007) is extended by Wang et al. (2007), Sarika et al. (2008), Wu et al. (2011), Nguyen et al. (2012), Wu et al. (2013), Huang et al. (2012), Song et al. (2014), Kissler et al. (2014) to develop control algorithms for exogenous insulin injections in artificial pancreas devices, applied by Strilka et al. (2014); Stull et al. (2016); Strilka et al. (2016) in studies of laboratory experiments for subcutaneous injection of insulin analogues, and also inspired theoretical analyses (Huard et al. 2015; Pei et al. 2011).

Clearly, insulin is a critical and necessary hormone for energy metabolism in humans. The insulin-degrading enzyme (IDE), also known as insulinolysin or insulin protease, is an enzyme, probably the most critical enzyme, to degrade and inactivate insulin action and many functions in the termination of the insulin response. Such activity is biologically important because of the limited half-life of the crucial hormone in humans (Broh-Kahn and Mirsky 1949). IDE deficiency leads to abundant insulin in circulation and further causes β -cell degeneration (Merino et al. 2020). Since the rate of insulin degradation at the cell level is basically determined by IDE activity, it is necessary to understand the relationship between improvements in IDE

activity and the occurrence and development of insulin resistance (IR). IDE is known as an inhibitor of type 2 diabetes therapeutics (Maianti et al. 2014; Pivovarov-Ramich et al. 2016). Some research has shown that IDE plays an important role in the degradation and clearance of insulin in cells, promotes insulin receptor recycling and new insulin secretion, and maintains a relatively stable insulin level in the body (Kuo et al. 1994; Gu et al. 2004; Tundo et al. 2017). The inhibitors of this activity may improve the action of insulin in rabbits was discovered in Mirsky et al. (1955). IDE mice have high insulin levels, but they show reduced glucose tolerance rather than increased, which may result from compensatory deficiency signaling of insulin (Farris et al. 2003; Abdul-Hay et al. 2011). Insulin is a biologically essential IDE substrate; abnormal insulin levels and inadequate insulin and other hormone responses that control glucose levels are the main causes of T2DM. According to the findings by Maianti et al. (2014), Farris et al. (2003), Malito et al. (2008), Shen et al. (2006), IDE as a disease susceptibility gene in both AD and T2DM. In the review (González-Casimiro et al. 2021), González-Casimiro et al. deliberated current knowledge about IDE’s function as a regulator of insulin secretion and hepatic insulin sensitivity and showed that IDE has an additional role in regulating hepatic insulin action and sensitivity through studying on mice with tissue-specific genetic deletion of IDE in the liver and pancreas β -cells. So it is worthwhile to investigate the impact of IDE in the regulation system. We refine the model in Li et al. (2006), Li and Kuang (2007) by involving the subtle processes regarding insulin degradation enzyme and study the inhibitory role of IDE in the degradation of insulin and glucagon in humans with the aim to elucidate certain intrinsic factors for IDE playing a critical role in the metabolic system.

We organize our paper as follows. In the next section, we carefully extend the two time delays model in Li et al. (2006), Li and Kuang (2007) by incorporating IDE according to physiology. In Sect. 3, we first show that the proposed model is well-posed and then investigate biological dynamical behaviors. When the analytical study is tedious and of limitation, we continue in Sect. 4 to numerically investigate the model behaviors within biological meaningful scopes. In Sect. 5, we will discuss our findings. The proofs of the main results are carried out in “Appendices”.

2 Model derivations

The two time delays model for the glucose-insulin regulatory system formulated by Li et al. (2006) with $G(t)$ and $I(t)$ stand for the glucose and insulin concentration at time t , respectively, is given as follows

$$\begin{cases} \frac{dG(t)}{dt} = G_{in} - f_2(G(t)) - f_3(G(t))f_4(I(t)) + f_5(I(t - \tau_2)), \\ \frac{dI(t)}{dt} = f_1(G(t - \tau_1)) - d_i I(t), \end{cases} \tag{1}$$

where the initial conditions are given by $G(t) \equiv G_0 > 0$ for $t \in [-\tau_1, 0]$ and $I(t) \equiv I_0 > 0$ for $t \in [-\tau_2, 0]$, $\tau_1, \tau_2 > 0$. The functions f_1 through f_5 are a set of highly non-linear and $d_i I$ is the insulin degradation with $d_i > 0$ as the constant

degradation rate. (The physiological meanings of each term will be explained below.) This has been studied by its original form or extended forms widely as stated as aforementioned in the last section.

In the case of the metabolism of hepatic IDE in mice (González-Casimiro et al. 2021), hepatic IDE overexpression will not alter insulin clearance, displaying that the pancreas decreased insulin production and secretion as a result of increased insulin sensitivity. This research evidences that in a preclinical mouse model of obesity and diabetes, reinforcing hepatic IDE function in the liver can regulate insulin resistance and glucose intolerance to some extent. Galagovsky et al. (2014) found that the highest *Drosophila* IDE (DIDE) /tubulin expression occurs in the fat body. They raised that DIDE is an insulin signaling modulator, and its loss of function promotes insulin resistance, a symptom of T2DM. Tsuda et al. (2010) shown that the overexpression of DIDE causes phenotypes that are presumably related to insulin deficiency. Now, we incorporate the functionalities of IDE on regulating insulin levels in this model and apply a function $\alpha(I)$ to capture the dynamic of IDE. Since the lack of a study on delay in activation of IDE due to insulin change, we try to take the time delay τ_3 in the insulin secretion to be equal to the amount of time that elapses before insulin secretion would respond to the changes in IDE.

In the second equation of model (1), Li et al. (2006) only considered the glucose concentration $G(t)$ as the sole stimuli ($f_1(G(t - \tau_1))$) to stimulate the production of insulin without the impact by IDE, where $\tau_1 > 0$ represents the time delay of the insulin response to the glucose stimulation and the time needed for the newly synthesized insulin crossing the endothelial barrier to become remote insulin. It is known that after insulin enters the liver through the portal vein, part of it is inactivated in the liver or re-enters the systemic circulation. Specifically, insulin enters the cell for degradation by IDE in the cytoplasm (Fawcett and Duckworth 2009). Excessive degradation of insulin in the cytoplasm can lead to a decrease in the amount of insulin that acts per unit of time and weaken the effect of insulin, thereby stimulating islet cells to secrete excessive insulin for compensation, which causes IR and hyperinsulinemia (Tandl and Kolb 1984; Abdul-Hay et al. 2011). IDE deficiency increases insulin secretion, which will eventually have deleterious effects on β -cell function leading to type 2 diabetes (Costes and Butler 2014; Fernández-Díaz et al. 2019). On the other hand, IDE overexpression improves glucose tolerance and insulin sensitivity, but, IDE overexpression in the liver does not affect insulin clearance (Merino et al. 2020). The work in Kukday et al. (2012) reveals that insulin is a dynamic factor impacting IDE effects. Dose-response studies reported in Fig. 4C by Kukday et al. (2012) reveal that IDE activity including insulin secretion over a range of human insulin (0–17.2 μM) follows a reverse Hill function kinetics with a tiny half-saturation value at 0.92 μM through data fitting. Thus, taking the impact of IDE on insulin secretion into account, we assume reasonably that the factor function $\alpha(I)$ satisfies the following assumptions:

- (A1): $\alpha(0) > 0$;
 (A2): $\alpha(I)|_{I>0} > 0$, $\frac{d\alpha(I)}{dI} < 0$, and $\lim_{I \rightarrow +\infty} \alpha(I) = 0$,

The shapes, rather than the form, of the response functions matter (Keener and Sneyd 2009). Thus, for the sake of convenience, we choose the multiplier $\alpha(I) := \frac{k_0 I(t)}{e^{cI} - 1}$, $k_0, c > 0$, where $k_0 I(t - \tau_3)$ represents the delayed effect of insulin degradation

product under the action of IDE on insulin secretion at time t , and the term $\frac{1}{e^{cI(t-\tau_3)} - 1}$ represents the probability of affecting the insulin secretion with time delay τ_3 , which correlates to the total amount of the biomass of insulin consumption with a constant $c > 0$. In which, $\alpha(0) = \frac{k_0}{c}$, and $\alpha(I) > 1$ indicates IDE deficiency, $\alpha(I) < 1$ stands for IDE overexpression, and $\alpha(I) = 1$ is for normal IDE level. Let $\hat{I} > 0$ be the unique value such that $\alpha(\hat{I}) = 1$. The above assumption can be described as: when the peripheral insulin is below \hat{I} , IDE is deficit; when the peripheral insulin is above \hat{I} , IDE is overexpressed. \hat{I} monotonically decreases when c increases.

According to the above physiological findings in rodents (Mirsky et al. 1955; Farris et al. 2003; Shen et al. 2006) and physiological observations discussed above, we extend Model (1) as below with the aim to investigate the links of defect in IDE with T2DM and/or AD in human. The novel model is given by

$$\begin{cases} \frac{dG(t)}{dt} = G_0 - f_2(G(t)) - f_3(G(t))f_4(I(t)) + f_5(I(t - \tau_2)), \\ \frac{dI(t)}{dt} = f_1(G(t - \tau_1))\frac{k_0I(t - \tau_3)}{e^{cI(t-\tau_3)} - 1} - d_1I(t), \end{cases} \tag{2}$$

where the constant glucose infusion term G_0 models the continuous intestinal glucose absorption after a meal or oral glucose. The diagram of this glucose-insulin model is shown in Fig. 1.

The function $f_1(G(t))$ is bounded and sigmoidal shape with $f_1(0) > 0$, $f_1(x) > 0$, $\frac{df_1(x)}{dx} > 0$ for $x > 0$. The functions $f_2(G(t))$ and $f_3(G(t))f_4(I(t))$ respectively denote the insulin-independent and insulin-dependent glucose utilization [see Li et al. (2006) for more details], where $f_2(x) > 0$ is in sigmoidal shape with $f_2(0) = 0$ and $\frac{df_2(x)}{dx} > 0$ is bounded for $x > 0$; $f_3(0) = 0$, $\frac{df_3(x)}{dx} > 0$ for $x > 0$; and $f_4(0) > 0$, $f_4(x) > 0$, $\frac{df_4(x)}{dx} > 0$ are bounded above for $x > 0$, $f_4(x)$ is in sigmoidal shape. Glucose production is denoted as $f_5(I(t))$ controlled by insulin concentration $I(t)$. $f_5(x)$ is in inverse sigmoidal shape, $f_5(0) > 0$, $f_5(x) > 0$, $\frac{df_5(x)}{dx} < 0$ for $x > 0$, and $f_5(x)$, $|\frac{df_5(x)}{dx}|$ are bounded above for $x > 0$. The function $f_5(I(t - \tau_2))$ represents the delayed HGP, indicating that the production is controlled by insulin with time delay $\tau_2 > 0$.

3 Stability analysis

In this section, we will focus on the existence of positive steady state solutions and local stability of the time-delay model (2). For simplicity, let $\tau_3 = \tau_2$.

Throughout this paper, we assume $f_i(x)$ ($i = 1, 2, 3, 4, 5$) satisfies the following conditions:

- (H1) $\lim_{x \rightarrow \infty} f_1(x) = M_1$, $f_1(0) := m_1 > 0$, $\frac{df_1(x)}{dx}$ is bounded by a constant $M'_1 > 0$ for $x > 0$;
- (H2) $\lim_{x \rightarrow \infty} f_2(x) = M_2$ and there exists a constant M'_2 such that $\frac{df_2(x)}{dx} < M'_2$ for $x > 0$;

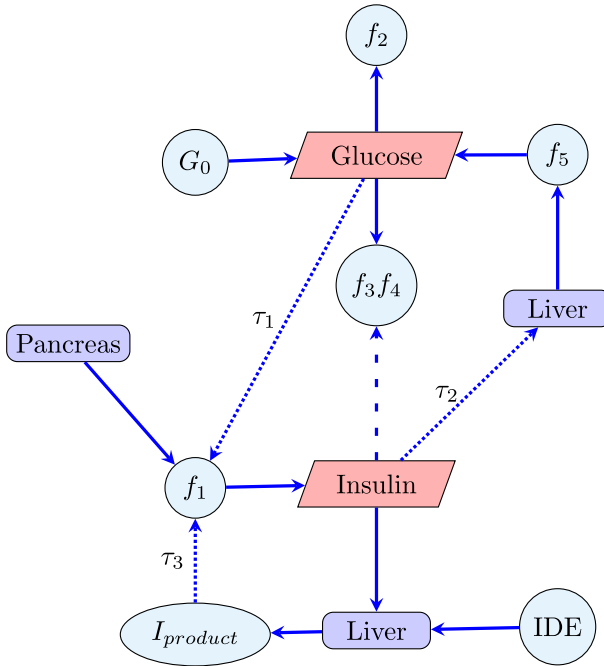


Fig. 1 Modeling framework showing the regulatory mechanisms. The functions represent f_1 —effect of glucose on insulin secretion, f_2 —insulin independent glucose utilization, $f_3 f_4$ —insulin dependent glucose utilization, and f_5 —effect of insulin on glucose production

- (H3) $f_4(0) := m_4 > 0$, there exist constants $M_3 > 0$, $M_4 > 0$ and $M'_4 > 0$ such that $0 < f_3(x) \leq M_3 x$, $\lim_{x \rightarrow \infty} f_4(x) = M_4$ and $\frac{df_4(x)}{dx} < M'_4$ for $x > 0$;
- (H4) $\lim_{x \rightarrow \infty} f_5(x) = 0$ and there exist constant $M_5, M'_5 > 0$ such that $f_5(x) \leq M_5$ and $|\frac{df_5(x)}{dx}| \leq M'_5$ for $x > 0$.

The boundedness of the solutions for the model (2) is presented in the following Proposition (the proof will be carried out in “Appendices”).

Proposition 3.1 For Model (2), the following hold:

- (i) If $\lim_{x \rightarrow \infty} f_3(x) > \frac{G_0 - M_2 + f_5(\frac{1}{c} \ln(k_0 M_1 + d_i))}{m_4}$, then Model (2) has a unique positive steady state (G^*, I^*) , where $I^* = \frac{1}{c} \ln(k_0 f_1(G^*) + d_i)$. Furthermore, all solutions are positive and bounded.
- (ii) If $\lim_{x \rightarrow \infty} f_3(x) < \frac{G_0 - M_2}{m_4}$, then $\limsup_{t \rightarrow \infty} G(t) = \infty$.

3.1 The case $\tau_1 \tau_2 = 0$

Although an explicit expression cannot be obtained, Model (2) possesses a unique steady state (G^*, I^*) , defined by the equations $\frac{dG(t)}{dt} = \frac{dI(t)}{dt} = 0$. In this subsection, we analyze the local stability of Model (2) at (G^*, I^*) in the case of $\tau_1 \tau_2 = 0$.

Letting $\widehat{G}(t) = G(t) - G^*$ and $\widehat{I}(t) = I(t) - I^*$, for simplicity we will not write the hat ($\widehat{}$) in the rest of this paper, then Model (2) is linearized around (G^*, I^*) as follows:

$$\begin{cases} \frac{dG(t)}{dt} = -W_1 G(t) - W_2 I(t) - W_3 I(t - \tau_2), \\ \frac{dI(t)}{dt} = W_4 G(t - \tau_1) - W_5 I(t - \tau_2) - d_i I(t). \end{cases} \tag{3}$$

Because f_1 through f_4 are monotonically increasing functions and f_5 is monotonically decreasing, it is easy to check that all the following parameters are positive,

$$\begin{cases} W_1 = \frac{d}{dG} f_2(G^*) + \frac{d}{dG} f_3(G^*) f_4(I^*) > 0, \\ W_2 = f_3(G^*) \frac{d}{dI} f_4(I^*) > 0, \\ W_3 = -\frac{d}{dI} f_5(I^*) > 0, \\ W_4 = \frac{d}{dG} f_1(G^*) \frac{k_0 I^*}{e^{cI^*} - 1} > 0, \\ W_5 = \frac{f_1(G^*) k_0 [(1 - cI^*) e^{cI^*} - 1]}{(e^{cI^*} - 1)^2} > 0. \end{cases} \tag{4}$$

The characteristic equation of (3) is

$$\begin{aligned} \mathcal{F}(\lambda) = \lambda^2 + (W_1 + W_5 e^{-\lambda \tau_2} + d_i) \lambda + W_1 d_i + W_2 W_4 e^{-\lambda \tau_1} \\ + W_1 W_5 e^{-\lambda \tau_2} + W_3 W_4 e^{-\lambda(\tau_1 + \tau_2)} = 0. \end{aligned} \tag{5}$$

For Model (2), the equilibrium point (G^*, I^*) will be asymptotically stable if all the roots of the characteristic equation (5) have negative real parts. In the case of a non-delayed model, we will assume that the equilibrium point (G^*, I^*) is asymptotically stable and then find conditions for which (G^*, I^*) is still asymptotically stable with all delays.

It is clear that $\mathcal{F}(0) = W_1(d_i + W_5) + (W_2 + W_3)W_4 > 0$, then $\lambda = 0$ is not a root of equation (5). Thus, if there is some stability switch of the trivial solution of the linearized model (3), there must be a pair of pure conjugate imaginary roots of Eq. (5). Equation (5) with $\tau_1 = \tau_2 = 0$ is equivalent to $\lambda^2 + (W_1 + W_5 + d_i)\lambda + W_1(d_i + W_5) + (W_2 + W_3)W_4 = 0$, we then have

Proposition 3.2 *Under the conditions $W_1 + W_5 + d_i > 0$ and $W_1(d_i + W_5) + (W_2 + W_3)W_4 > 0$, the steady state solution (G^*, I^*) of Model (2) with $\tau_1 = \tau_2 = 0$ is asymptotically stable.*

When $\tau_1 > 0$ and $\tau_2 = 0$, Eq. (5) is equivalent to

$$\mathcal{F}(\lambda) = \lambda^2 + (W_1 + W_5 + d_i)\lambda + W_1(d_i + W_5) + (W_2 + W_3)W_4 e^{-\lambda \tau_1} = 0. \tag{6}$$

Referring to Lemma 4.1 in Li and Kuang (2007), we get $2W_1(d_i + W_5) - (W_1 + W_5 + d_i)^2 = -(W_1^2 + (W_5 + d_i)^2) < 0$ and state the following results without proofs.

Proposition 3.3 *For Model (2) with $\tau_1 > 0$ and $\tau_2 = 0$,*

- (i) If $W_1(d_i + W_5) > (W_2 + W_3)W_4$, then the positive stationary solution (G^*, I^*) of model (2) is always stable for $\tau_1 > 0$;
- (ii) If $W_1(d_i + W_5) < (W_2 + W_3)W_4$, there exists a constant $\tau_1^0 > 0$ such that (G^*, I^*) of model (2) is stable for $\tau_1 \in (0, \tau_1^0)$ and unstable for $\tau_1 > \tau_1^0$. A Hopf bifurcation occurs as τ_1 passes through the critical value τ_1^0 .

When $\tau_1 = 0$ and $\tau_2 > 0$, Eq. (5) is equivalent to

$$\mathcal{F}(\lambda) = \lambda^2 + (W_1 + d_i + W_5 e^{-\lambda\tau_2})\lambda + W_1 d_i + W_2 W_4 + (W_1 W_5 + W_3 W_4) e^{-\lambda\tau_2} = 0. \quad (7)$$

Let

$$\begin{cases} A = W_1 + d_i > 0, \\ B = W_5 > 0, \\ C = W_1 W_5 + W_3 W_4 > 0, \\ D = W_1 d_i + W_2 W_4 > 0, \end{cases} \quad (8)$$

then Eq. (7) becomes

$$\mathcal{F}(\lambda) = \lambda^2 + A\lambda + B\lambda e^{-\lambda\tau_2} + D + C e^{-\lambda\tau_2} = 0. \quad (9)$$

Applying the Lemma in Cooke and Grossman (1982), Wei and Ruan (1999), we deduce the following results and the proof can be found in ‘‘Appendices’’.

Lemma 3.1 For Eq. (9), we have

- (i) If $D < C$ holds and $\tau_2 = \tau_2^{n,1}$, then Eq. (9) has a pair of purely imaginary roots $\pm i\omega_+$;
- (ii) If $(A^2 - B^2 - 2D)^2 > 4(D + C)(D - C) > 0 > A^2 - B^2 - 2D$ holds and $\tau_2 = \tau_2^{n,1}$ (res. $\tau_2 = \tau_2^{n,2}$), then Eq. (9) has a pair of purely imaginary roots $\pm i\omega_+$ (res. $\pm i\omega_-$);
- (iii) If neither $D < C$ nor $(A^2 - B^2 - 2D)^2 > 4(D + C)(D - C) > 0 > A^2 - B^2 - 2D$ and $\tau_2 > 0$, then Eq. (9) has no purely imaginary root, where

$$\begin{aligned} \omega_{\pm}^2 &= \frac{-(A^2 - B^2 - 2D) \pm \sqrt{(A^2 - B^2 - 2D)^2 - 4(D + C)(D - C)}}{2}, \\ \tau_2^{n,1} &= \frac{1}{\omega_+} \left[\arccos \left(\frac{C(\omega_+^2 - D) - AB\omega_+^2}{C^2 + B^2\omega_+^2} \right) + 2n\pi \right], \\ \tau_2^{n,2} &= \frac{1}{\omega_-} \left[\arccos \left(\frac{C(\omega_-^2 - D) - AB\omega_-^2}{C^2 + B^2\omega_-^2} \right) + 2n\pi \right], \quad n = 0, 1, \dots \end{aligned} \quad (10)$$

Consider the characteristic roots of Eq. (9) as

$$\lambda_{k,n}(\tau_2) = \alpha_{k,n}(\tau_2) + i\omega_{k,n}(\tau_2), \quad k = 1, 2; \quad n = 0, 1, \dots \quad (11)$$

where

$$\alpha_{1,n}(\tau_2^{n,1}) = 0, \quad \omega_{1,n}(\tau_2^{n,1}) = \omega_+ \tag{12}$$

and

$$\alpha_{1,n}(\tau_2^{n,2}) = 0, \quad \omega_{2,n}(\tau_2^{n,2}) = \omega_- \tag{13}$$

It can be verified that the following lemma is true.

Lemma 3.2 *Let $\tau_2^{n,k}$ ($k = 1, 2$) associated with $\omega_{k,n}$. For $\tau_2 = \tau_2^{n,k}$, the characteristic Eq. (9) has a pair purely imaginary roots $\pm i\omega_{k,n}$, satisfying*

$$\text{sign} \left\{ \left. \frac{d\text{Re}(\lambda)}{d\tau_2} \right|_{\tau_2 = \tau_2^{n,k}} \right\} = \text{sign} \{ A^2 - B^2 - 2D + 2\omega_{k,n}^2 \},$$

where $\tau_2^{n,k}$ and $\omega_{k,n}$ are defined in Eqs. (10), (12) and (13).

The proof of Lemma 3.2 is attached in ‘‘Appendices’’.

Thus, applying the Lemma in Wei and Ruan (1999), we obtain the distribution of the characteristic roots of Eq. (9).

Lemma 3.3 *For Eq. (9), we have the following*

- (i) *If $D < C$ holds, then when $\tau_2 \in [0, \tau_2^{0,1})$ all roots of Eq. (9) have negative real parts, and when $\tau_2 > \tau_2^{0,1}$ Eq. (9) has at least one root with positive real part.*
- (ii) *If $(A^2 - B^2 - 2D)^2 > 4(D + C)(D - C) > 0 > A^2 - B^2 - 2D$ holds, then there are j switches from stability to instability, that is, when $\tau_2 \in (\tau_2^{n,2}, \tau_2^{n+1,1})$ ($n = -1, 0, 1, \dots, j - 1$), all roots of Eq. (9) have negative real parts, where $\tau_2^{-1,2} = 0$, and when $\tau_2 \in [\tau_2^{n,1}, \tau_2^{n,2})$ and $\tau_2 > \tau_2^{j,1}$ ($n = 0, 1, \dots, j - 1$), Eq. (9) has at least one root with positive real part.*

Based on the above analysis, we thus obtain the following results on the stability of the steady state solution (G^*, I^*) of Model (2).

Theorem 3.1 *For Model (2), the number of different imaginary roots with positive (negative) imaginary parts of Eq. (9) can be zero, one, or two only.*

- (i) *If $D > C$ and $A^2 - B^2 - 2D > 0$ hold, then the stability of the steady state solution (G^*, I^*) does not change for all $\tau_2 > 0$.*
- (ii) *If $D < C$ holds, there is one imaginary root with a positive imaginary part, an unstable steady state solution (G^*, I^*) never becomes stable for any $\tau_2 > 0$. If the steady state solution (G^*, I^*) is asymptotically stable for $\tau_2 = 0$, then it is uniformly asymptotically stable for $0 < \tau_2 < \tau_2^{0,1}$, and it becomes unstable for $\tau_2 > \tau_2^{0,1}$. A Hopf bifurcation occurs as τ_2 passes through the critical value $\tau_2^{0,1}$, where $\tau_2^{0,1}$ is given in (10).*

(iii) If $(A^2 - B^2 - 2D)^2 > 4(D + C)(D - C) > 0 > A^2 - B^2 - 2D$ holds, there are two imaginary roots with positive imaginary part, $i\omega_+$ and $i\omega_-$, such that $\omega_+ > \omega_- > 0$, then the stability of the steady state solution (G^*, I^*) can change a finite number of times at most as τ_2 is increased, and eventually it becomes unstable.

Remark 1 See the ‘‘Appendices’’ for the detailed proof of Theorem 3.1. From Theorem 3.1, it is easy to find that Model (2) undergoes a Hopf bifurcation related not only to the value of τ_2 but also to the value of the rate of insulin release k_0 . We shall demonstrate numerical investigation in Sect. 4.

3.2 The case $\tau_1\tau_2 \neq 0$

In this subsection, we assume both $\tau_1 > 0$ and $\tau_2 > 0$. We first let $\tau_1 = \tau_2 = \tau$, Eq. (5) equals to

$$\lambda^2 + (W_1 + d_i)\lambda + W_1d_i + (W_5\lambda + W_2W_4 + W_1W_5 + W_3W_4e^{-\lambda\tau})e^{-\lambda\tau} = 0, \tag{14}$$

and $\lambda = 0$ is not a characteristic root of Eq. (14). Set

$$\begin{aligned} \Phi(\lambda, \tau) &:= \lambda^2 + (W_1 + d_i)\lambda + W_1d_i, \\ \Psi(\lambda, \tau) &:= W_5\lambda + W_2W_4 + W_1W_5 + W_3W_4e^{-\lambda\tau}, \end{aligned} \tag{15}$$

we consider $\lambda = i\omega$ is a root of the characteristic Eq. (14), where ω is assumed to be strictly greater than 0. From (15), we denote by Φ_R, Ψ_R the real parts of Φ, Ψ , and by Φ_I, Ψ_I the imaginary parts of Φ, Ψ , respectively. Thus, $\Phi_R(i\omega, \tau) = W_1d_i - \omega^2, \Phi_I(i\omega, \tau) = (W_1 + d_i)\omega, \Psi_R(i\omega, \tau) = W_1W_5 + W_2W_4 + W_3W_4 \cos \omega\tau, \Psi_I(i\omega, \tau) = W_5\omega - W_3W_4 \sin \omega\tau$. Therefore, ω satisfies the following equations,

$$\begin{cases} \Psi_I(i\omega, \tau) \sin \omega\tau + \Psi_R(i\omega, \tau) \cos \omega\tau = -\Phi_R(i\omega, \tau), \\ \Psi_I(i\omega, \tau) \cos \omega\tau - \Psi_R(i\omega, \tau) \sin \omega\tau = -\Phi_I(i\omega, \tau), \end{cases} \tag{16}$$

which gives

$$\begin{aligned} \sin \omega\tau &= \frac{-\Phi_R(i\omega, \tau)\Psi_I(i\omega, \tau) + \Phi_I(i\omega, \tau)\Psi_R(i\omega, \tau)}{\Psi_R^2(i\omega, \tau) + \Psi_I^2(i\omega, \tau)} = \text{Im} \left(\frac{\Phi(i\omega, \tau)}{\Psi(i\omega, \tau)} \right), \\ \cos \omega\tau &= -\frac{\Phi_R(i\omega, \tau)\Psi_R(i\omega, \tau) + \Phi_I(i\omega, \tau)\Psi_I(i\omega, \tau)}{\Psi_R^2(i\omega, \tau) + \Psi_I^2(i\omega, \tau)} = -\text{Re} \left(\frac{\Phi(i\omega, \tau)}{\Psi(i\omega, \tau)} \right). \end{aligned} \tag{17}$$

Then, we derive

$$\begin{aligned} \mathfrak{F}(\omega, \tau) &= |\Phi(i\omega, \tau)|^2 - |\Psi(i\omega, \tau)|^2 \\ &= \omega^4 + (W_1^2 + d_i^2 - W_5^2)\omega^2 + 2\omega W_3W_4W_5 \sin \omega\tau + W_1^2d_i^2 - W_3^2W_4^2 \\ &\quad - (W_2W_4 + W_1W_5)^2 - 2(W_2W_4 + W_1W_5)W_3W_4 \cos \omega\tau, \end{aligned} \tag{18}$$

and ω satisfies the transcendental equation $\mathfrak{F}(\omega, \tau) = 0$ which implies

$$\omega^4 + (W_1^2 + d_i^2 - W_5^2)\omega^2 + W_1^2 d_i^2 - W_3^2 W_4^2 - (W_2 W_4 + W_1 W_5)^2 = 2(W_2 W_4 + W_1 W_5)W_3 W_4 \cos \omega\tau - 2\omega W_3 W_4 W_5 \sin \omega\tau. \tag{19}$$

If $\omega = 0$, we check that

$$\mathfrak{F}(0) = W_1^2 d_i^2 - W_3^2 W_4^2 - (W_2 W_4 + W_1 W_5)^2 - 2(W_2 W_4 + W_1 W_5)W_3 W_4, \tag{20}$$

when $W_1^2 d_i^2 < W_3^2 W_4^2 + (W_2 W_4 + W_1 W_5)(W_2 W_4 + W_1 W_5 + 2W_3 W_4)$, then $\mathfrak{F}(0) < 0$. Also, it is easy to check that $\mathfrak{F}(+\infty) > 0$, so we can obtain that Eq. (19) has finite positive roots.

Let us define $\phi(\tau) \in [0, 2\pi]$ such that

$$\begin{aligned} \sin \phi(\tau) &= \frac{-(W_1 d_i - \omega^2)(W_5 \omega - W_3 W_4 \sin \omega\tau) + \omega(W_1 + d_i)(W_2 W_4 + W_1 W_5 + W_3 W_4 \cos \omega\tau)}{(W_2 W_4 + W_1 W_5 + W_3 W_4 \cos \omega\tau)^2 + (W_5 \omega - W_3 W_4 \sin \omega\tau)^2}, \\ \cos \phi(\tau) &= -\frac{(W_1 d_i - \omega^2)(W_2 W_4 + W_1 W_5 + W_3 W_4 \cos \omega\tau) + \omega(W_1 + d_i)(W_5 \omega - W_3 W_4 \sin \omega\tau)}{(W_2 W_4 + W_1 W_5 + W_3 W_4 \cos \omega\tau)^2 + (W_5 \omega - W_3 W_4 \sin \omega\tau)^2}, \end{aligned} \tag{21}$$

where $\phi(\tau) = \omega\tau - 2n\pi$, $n \in \mathbb{N}_0$. Define the maps τ_n given by

$$\tau_n(\tau) := \frac{\phi(\tau) + 2n\pi}{\omega}, \quad n \in \mathbb{N}_0, \tag{22}$$

where ω is a positive root of Eq. (19). Then, Eq. (21) jointly with (19) defines the functions

$$\Gamma_n(\tau) := \tau - \tau_n(\tau), \quad n \in \mathbb{N}_0, \tag{23}$$

which are continuous and differentiable. From (18) we have

$$\begin{aligned} \frac{d\mathfrak{F}(\omega, \tau)}{d\omega} &= 4\omega^3 + 2(W_1^2 + d_i^2 - W_5^2)\omega + 2W_3 W_4 W_5 \sin \omega\tau \\ &\quad + 2\tau W_3 W_4 (\omega W_5 \cos \omega\tau + (W_2 W_4 + W_1 W_5) \sin \omega\tau). \end{aligned} \tag{24}$$

By virtue of Beretta and Kuang (2002) and Kuang (2012), we set the following results.

Theorem 3.2 *Assume that ω is a positive real root of Eq. (19) and there exist some positive constants τ^* such that $\Gamma_n(\tau^*) = 0$ for some $n \in \mathbb{N}_0$. Then a pair of simple conjugate pure imaginary roots $\lambda_{\pm}(\tau^*) = \pm i\omega(\tau^*)$ of Eq. (14) exists at $\tau = \tau^*$ which crosses the imaginary axis from left to right if $\Theta(\tau^*) > 0$ and crosses the imaginary axis from right to left if $\Theta(\tau^*) < 0$, where*

$$\begin{aligned} \Theta(\tau^*) &= \text{sign} \left\{ \left. \frac{d\text{Re}(\lambda)}{d\tau} \right|_{\lambda=i\omega(\tau^*)} \right\} \\ &= \text{sign} \left\{ \frac{d}{d\omega} \mathfrak{F}(\omega(\tau^*), \tau^*) \right\} \text{sign} \left\{ \left. \frac{d\Gamma_n(\tau)}{d\tau} \right|_{\tau=\tau^*} \right\}. \end{aligned} \tag{25}$$

In the following, we consider the case where $\tau_1 \neq \tau_2$ ($\tau_1 > 0, \tau_2 > 0$). For the characteristic equation of (3)

$$\begin{aligned} \mathcal{F}(\lambda) = & \lambda^2 + (W_1 + d_i)\lambda + W_1d_i + (\lambda + W_1)W_5e^{-\lambda\tau_2} + W_2W_4e^{-\lambda\tau_1} \\ & + W_3W_4e^{-\lambda(\tau_1+\tau_2)} = 0, \end{aligned} \tag{26}$$

we set

$$\begin{aligned} \mathbf{f}(\lambda) := & \lambda^2 + (W_1 + d_i)\lambda + W_1d_i, \\ \mathbf{g}(\lambda) := & (\lambda + W_1)W_5e^{-\lambda\tau_2} + W_2W_4e^{-\lambda\tau_1} + W_3W_4e^{-\lambda(\tau_1+\tau_2)}. \end{aligned} \tag{27}$$

Applying Rouchè’s theorem, we get the following result.

Theorem 3.3 *For Model (2), the characteristic Eq. (26) with $W_i > 0$ ($i = 1, 2, 3, 4, 5$) and assume that*

- (i) $\tau_2 - \tau_1 \leq \frac{1}{W_1} \ln \frac{W_2W_4 + W_3W_4}{\omega_0W_5}$;
- (ii) $W_1W_5 + W_2W_4 > W_3W_4$,

then there exists a constant $r_0 > 0$ such that $r_0^2 + (W_1 + d_i)r_0 + W_1d_i < \min \left\{ \frac{W_1W_5 + W_2W_4}{2}, W_1W_5 + W_2W_4 - W_3W_4 \right\}$, Eq. (26) has at least one root with negative real part for all $0 < r < r_0$.

Remark 2 The details about the proof of Theorem 3.3 are given in “Appendix”. In the case when $\tau_1\tau_2 > 0$, it can be obtained that for any given $\tau_1 > 0$, there exists $\tau_2(\tau_1) > 0$ such that a Hopf bifurcation occurs at (τ_1, τ_2) . Mathematically, Model (2) allows the interaction of unstable modes, but this tends to occur only with large delay values.

When considering Eq. (26) with τ_2 in its stable intervals, we take τ_1 into consideration as a parameter in accordance with Ruan and Wei’s method (Wei and Ruan 1999; Ruan and Wei 2003) and arrive at the following lemma regarding the sign of the real parts of characteristic roots of (26). The proof of the lemma is shown in “Appendices”.

Lemma 3.4 *Assume that all roots of Eq. (9) have negative real parts for $\tau_2 > 0$, then there exists a $\tau_1^*(\tau_2) > 0$ such that all roots of Eq. (26) have negative real parts if $0 < \tau_1 < \tau_1^*(\tau_2)$.*

From Theorem 3.1, notice that all roots of Eq. (9) have negative real parts when $0 < \tau_2 < \tau_2^{0,1}$ ($\tau_2^{0,1}$ is given in Eq. (10)), then we obtain the following asymptotic stability of the steady state (G^*, I^*) of Model (2).

Theorem 3.4 *Assume that $D < C$ or $(A^2 - B^2 - 2D)^2 > 4(D + C)(D - C) > 0 > A^2 - B^2 - 2D$ holds, for any $0 < \tau_2 < \tau_2^{0,1}$, there is a $\tau_1^*(\tau_2) > 0$ such that the steady state (G^*, I^*) of Model (2) is locally asymptotically stable when $0 < \tau_2 < \tau_1^*(\tau_2)$, where $\tau_2^{0,1}$ is taken as Eq. (10).*

Table 1 Functions and parameters values used for simulation of Model (2)

Function	Estimate/ Units	Reference
$f_1 = R_1 \arctan \left(\frac{G}{C_1 + V_1} \right)^2 + a_1$	$R_1 = 24 \mu\text{U}/\text{min}$ $C_1 = 58.82 \text{ mg}/\text{l}$ $V_1 = 101$ $a_1 = 2.3 \mu\text{U}/\text{min}$	Estimated
$f_2 = R_2 \arctan \left(\frac{G^\beta}{C_2 V_2} + 1 \right)^2 - a_2$	$R_2 = 4 \text{ mg}/\text{min}$ $\beta = 1.08$ $C_2 = 300 \text{ mg}/\text{l}$ $V_2 = 101$ $a_2 = \pi \text{ mg}/\text{min}$	Estimated
$f_3 = \frac{G}{C_3 V_3}$	$C_3 = 10 \text{ mg}/\text{l}$ $V_3 = 101$	Li and Kuang (2007)
$f_4 = R_4 \arctan \left(\frac{I + U_i}{C_4 V_4} \right)^2$	$R_4 = 30 \text{ mg}/\text{min}$ $U_i = 300 \mu\text{U}$ $C_4 = 100 \mu\text{U}/\text{l}$ $V_4 = 101$	Estimated
$f_5 = R_5 \left(\frac{\pi}{2} - \arctan(a_5(I - C_5)) \right)$	$R_5 = 1 \text{ mg}/\text{min}$ $a_5 = 0.4$ $C_5 = 20 \text{ mg}$	Estimated
$I DE = \frac{I}{e^{cI} - 1}$	$c = 0.06$	Estimated

4 Numerical simulations

In this section, we present numerical analysis to investigate the model (2) behaviors. The functions and parameters we use are listed in Table 1.

4.1 Effects of the two time delays τ_1 and τ_2

By opting the time delays τ_1, τ_2 as bifurcation parameters and fixing other parameters as given in Table 1, we investigate the influence of τ_1 and τ_2 on the glucose-insulin regulatory system and analyze the relationship between the two delays while $G_0 = 1.35 \text{ (mg/dl/min)}$, $d_i = 0.1$ and the insulin degradation rate $k_0 = 0.1 \text{ (/min)}$ are fixed.

The top and bottom meshes in Fig. 2 demonstrate the amplitudes of glucose and insulin concentrations, respectively. Figure 2 shows that a complex curve divides $[0, 100] \times [0, 100]$ in the (τ_1, τ_2) -plane into two regions. The steady state is stable in one region and unstable in the other. From the figure, glucose and insulin concentrations have larger amplitudes when the insulin response delay τ_1 is small and the HGP delay τ_2 is big.

Fig. 2 Amplitudes of glucose (top) and insulin (bottom) concentrations when τ_1 and τ_2 vary, where $G_0 = 1.35$ (mg/dl/min), $d_i = 0.1$, $k_0 = 0.1$ (/min) are fixed. Rest of the parameters values are given in Table 1

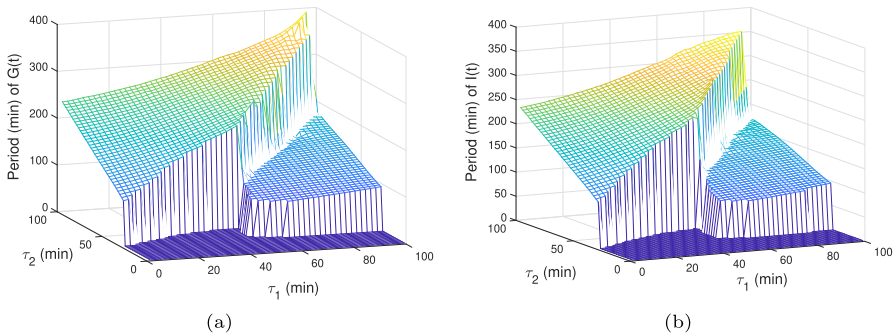
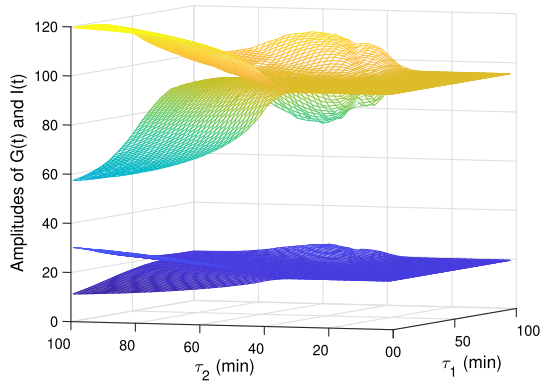


Fig. 3 Period of the glucose concentration (a) and insulin concentration (b), where $G_0 = 1.35$, $d_i = 0.1$, $k_0 = 0.1$ are fixed. All other parameters are given in Table 1

Glucose and insulin concentrations have amplitudes of (50, 120) and (10, 35), respectively when $\tau_2 \in (30, 100)$ with increasing the value of τ_1 .

Figure 3a, b show the period variations of glucose concentration and insulin concentration with respect to the time delays τ_1 and τ_2 for G_0 fixed at 1.35 and $k_0 = 0.1$, $d_i = 0.1$, respectively. There are sudden jumps in glucose and insulin concentration amplitudes when $\tau_1 > 60$ and $\tau_2 > 40$ approximately. In such cases, the periods of periodic solutions will decrease with increasing the values of τ_1 and τ_2 . Longer τ_1 and τ_2 would increase the oscillation period of the dynamic system and result in higher glucose concentration.

We let both τ_1 and τ_2 vary simultaneously and investigate the codimension-two bifurcation. Figure 4 displays that a bifurcation curve in the window $[0, 50] \times [0, 100]$ divides the (τ_1, τ_2) -plane into two regions, in one of the regions the equilibrium point is stable and in the other one a limit cycle exists. Moreover, we calculate that the Hopf bifurcation occurs at (G^*, I^*) when $\tau_1 = 0$ for τ_2 about 30 min. The oscillating solutions are observed for τ_2 values higher than the critical value.

Figure 5 exhibits the profiles obtained from the time delay model (2) with different parameter values. Figure 5a, b show the corresponding time evolution and phase diagram of glucose and insulin concentrations at $(\tau_1, \tau_2) = (10, 60)$ and $(\tau_1, \tau_2) = (10, 100)$, respectively. For both the glucose (the blue line) and the insulin

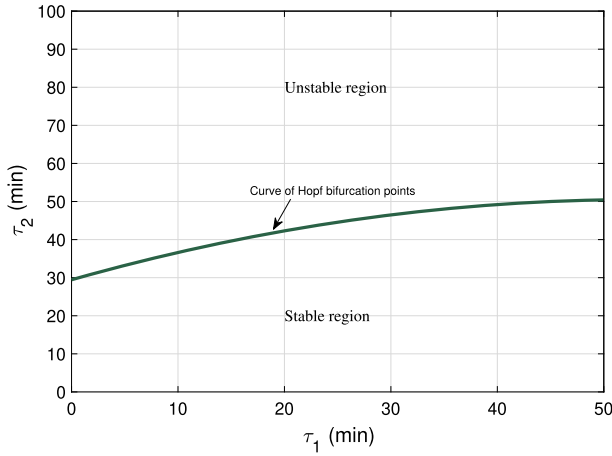


Fig. 4 Codimension-two bifurcation diagram, where $G_0 = 1.35$, $k_0 = 0.1$, $d_i = 0.1$ are fixed. Rest of the parameters are the same as in Table 1

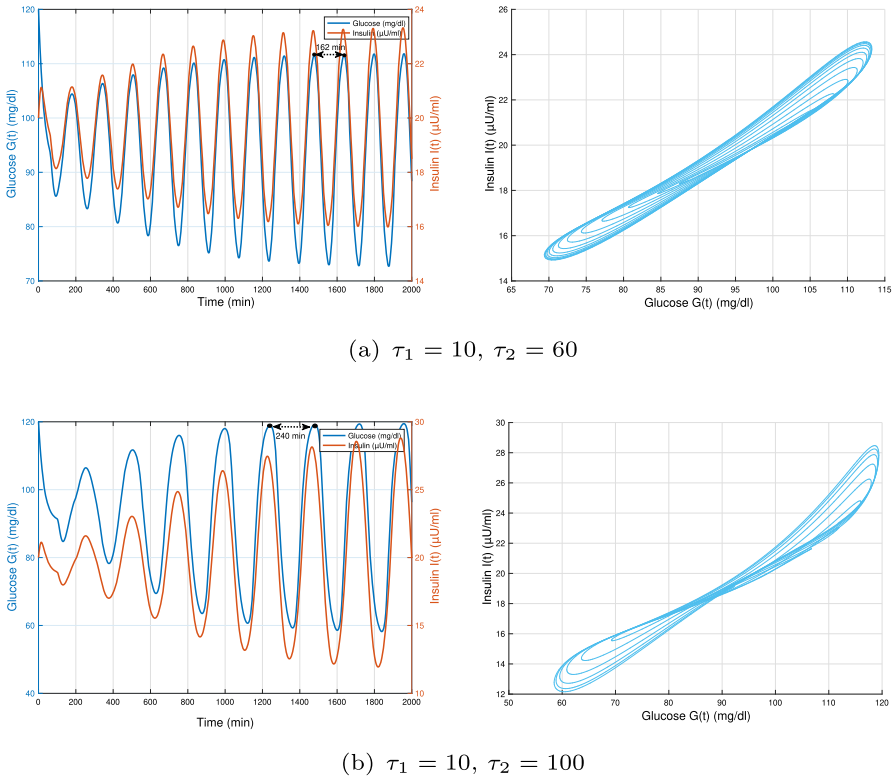


Fig. 5 Time series and phase diagram of glucose and insulin in Model (2). The time delays are **a** $(\tau_1, \tau_2) = (10, 60)$ and **b** $(\tau_1, \tau_2) = (10, 100)$, where $G_0 = 1.35$, $k_0 = 0.1$, $d_i = 0.1$ are fixed. All other parameters are given in Table 1

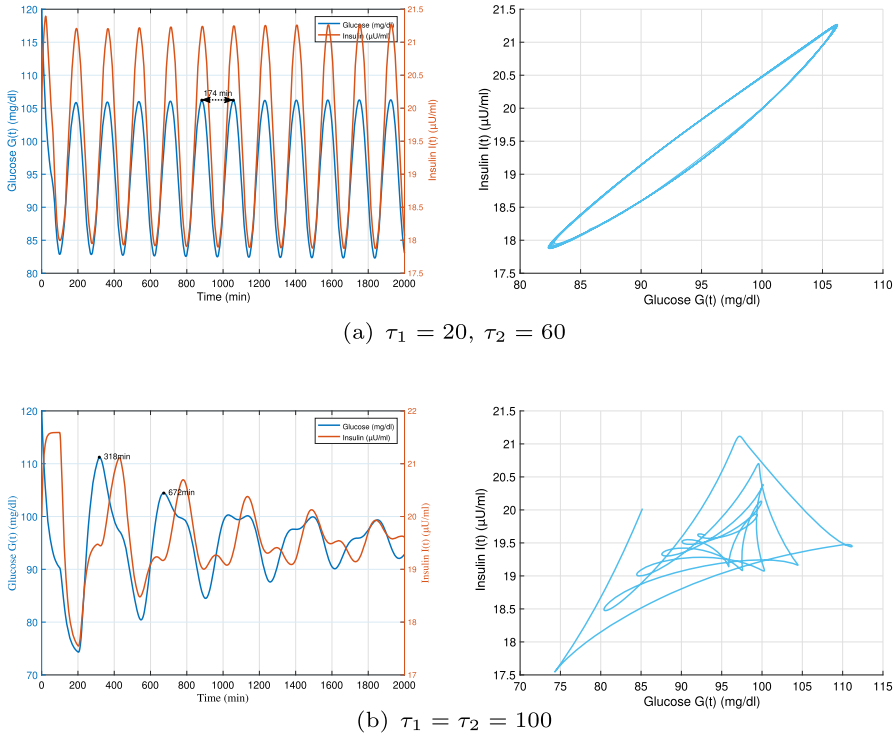


Fig. 6 Time series and phase diagram of glucose and insulin in Model (2). The time delays are **a** $(\tau_1, \tau_2) = (20, 60)$ and **b** $(\tau_1, \tau_2) = (100, 100)$, where $G_0 = 1.35, k_0 = 0.1, d_i = 0.1$ are fixed. All other parameters are given in Table 1

(the red line), oscillating solutions are visible with periods of approximately 162 min (see Fig. 5a). This periodic solution can be regarded as the sustained oscillation of glucose and insulin concentrations. The steady state (G^*, I^*) of Model (2) is unstable in this case. We get oscillations with longer periods—about 240 min—when τ_2 continues to rise above the critical value (see Fig. 5b). For instance, we can see that every 240 min, the glucose concentration drops to very low levels and the varying range of glucose concentration is scope [58, 119]. It should be noted that as τ_2 increases, the amplitudes of the oscillations of the glucose $G(t)$ and insulin $I(t)$ grow.

When τ_1 is destabilized and elevated, longer periods for both glucose and insulin can be seen. Figure 6a illustrates the solutions of the model (2) for the time delays $\tau_1 = 20$ and $\tau_2 = 60$ with periods of about 174 min. It also depicts a phase space project of two coexisting stable periodic solutions on (G, I) for $(\tau_1, \tau_2) = (20, 60)$. Chaotic behavior is shown in Fig. 6b which could explain the observed irregular oscillations of glucose and insulin concentrations. It confirms that the glucose level in an early time becomes higher and the oscillations become damped when the delays τ_1 and τ_2 become longer. Figure 6 displays that the occurrence and properties of oscillations are dependent on the magnitude of time delays. In addition, the duration time at the first high peak as $G > 100 \text{ mg/dl}$ in Fig. 6a is 190 min. It is shorter than all two peaks

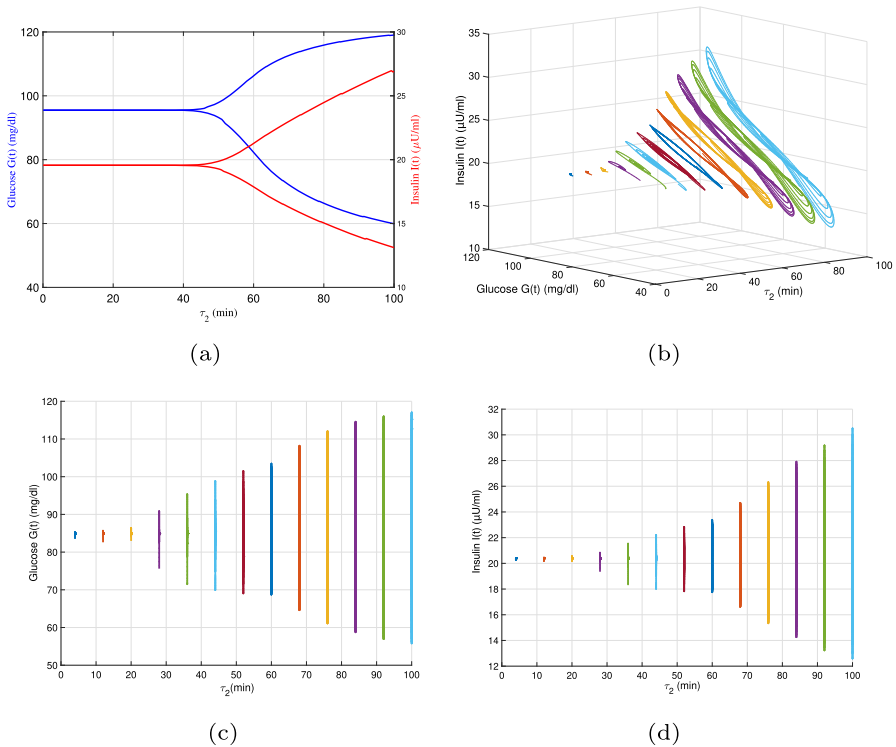


Fig. 7 **a** Hopf bifurcation diagram for values of τ_2 , **b** the phase portrait of glucose and insulin level with values of τ_2 , **c**, **d** the glucose and insulin level distributions for values of τ_2 , respectively, where $\tau_1 = 20$, $G_0 = 1.35$, $k_0 = 0.1$, $d_i = 0.1$ are fixed. All other parameters are given in Table 1

in Fig. 6b which spend 318 min and 672 min, respectively, to return the glucose level $G = 100 \text{ mg/dl}$.

4.2 Effects of the time delay τ_1 or τ_2 , the insulin degradation rate k_0 and glucose infusion rate G_0

In order to illustrate the model dynamics and the evolution of solutions, we change four parameters to reveal the Hopf bifurcation dynamics. The parameters that will be chosen are the time delays (τ_1 and τ_2), the exogenous glucose infusion rate G_0 , and the insulin degradation rate k_0 .

Figure 7a, b show the bifurcation diagram and phase portrait for varying $\tau_2 \in [0, 100]$ and fixing $\tau_1 = 20$, $G_0 = 1.35$, $k_0 = 0.1$, $d_i = 0.1$. A critical value of τ_2 to sustain the oscillation is found to be about 45 min (see Fig. 7a). For τ_2 shorter than 45 min, the oscillations are damped quickly. This shows that for values of τ_2 less than the critical value for which a Hopf bifurcation occurs (i.e., $\tau_2^{0,1}$, as stated in Theorem 3.1), then (G^*, I^*) is asymptotically stable for small values of τ_1 (see Theorem 3.4). It can be seen from Fig. 7b that our model is also capable of reproducing

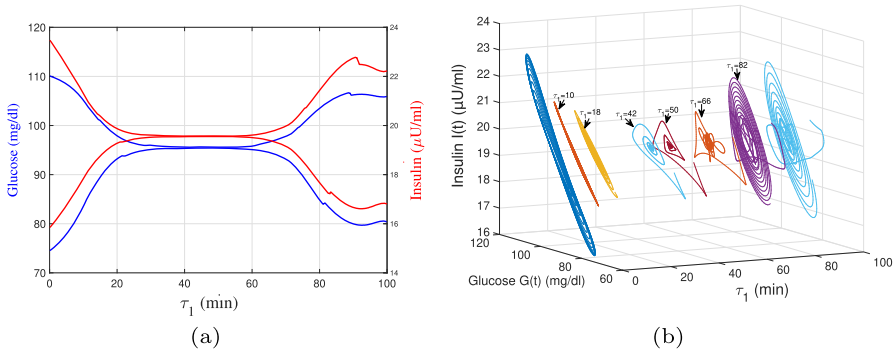


Fig. 8 **a** Hopf bifurcation diagram for values of τ_1 and **b** the phase portrait of glucose and insulin level with values of τ_1 , where $\tau_2 = 50$, $G_0 = 1.35$, $k_0 = 0.1$, $d_i = 0.1$ are fixed. All other parameters are given in Table 1

sustainable oscillations for different values of τ_2 . A range of τ_2 is estimated at 45 – 100 to sustain the oscillation of Model (2) when $\tau_1 = 20$ is fixed (see Fig. 7b). The oscillation orbits gradually grow into large-sized with increasing the value of τ_2 . Figure 7c, d are respectively the phase planes of glucose and insulin concentrations among various values of $\tau_2 \in [0, 100]$. The observation indicates that both glucose and insulin fluctuations become more significant with a longer delay.

A similar procedure is applied to analyzing the time delay τ_1 . Figure 8a, b show the bifurcation diagram and phase portrait for $\tau_2 = 50$, $G_0 = 1.35$, $k_0 = 0.1$, $d_i = 0.1$ and varying $\tau_1 \in [0, 100]$. For τ_1 out of the ranges of 0 – 40 and 50 – 100, the oscillations of glucose and insulin are damped when $\tau_2 = 50$ is fixed (see Fig. 8b). For τ_1 greater than 40 and less than 50, the glucose-insulin system reached a steady state quickly. For τ_1 in the 0–40 and 50–100 range, glucose concentration is changing within the optimal range.

We define the rate of insulin degradation k_0 to illustrate the effect of IDE, the degradative process may also be involved in mediating some aspects of insulin action. Fixing $\tau_1 = 20$, $\tau_2 = 60$ and $G_0 = 1.35$, $d_i = 0.1$, Fig. 9a shows the bifurcation diagram for the parameter range $k_0 \in [0, 0.15]$. For k_0 greater than 0.09, the glucose and insulin concentrations hardly change. The phase plane diagram for k_0 at Fig. 9b exhibits the oscillation variation behavior. An optimal range of k_0 is estimated at 0.01 – 0.15 for the periodic solution of the dynamics system (see Fig. 9b). When k_0 increased from 0 to 0.15, glucose and insulin concentrations change stably within the normal ranges. The magnitude of glucose level is between 82 and 107 responds to $k_0 \in [0, 0.15]$ at Fig. 9c with $\tau_1 = 20$ and $\tau_2 = 60$. The range of insulin concentrations is between 17.5 and 21.5 as the parameter k_0 located in $[0, 0.15]$ according to Fig. 9d. This indicates a good degree of stability in the inter-regulation of the glucose-insulin system.

Taking both the glucose infusion rate G_0 and the insulin degradation rate k_0 as bifurcation parameters while $\tau_1 = 25$, $\tau_2 = 50$ and $d_i = 0.1$ are fixed, we identify the stability regions in $(k_0, G_0) \in [0, 0.15] \times [0, 2]$. Figure 10 displays that a simple curve divides the rectangular $(k_0, G_0) \in [0, 0.15] \times [0, 2]$ into two regions. The steady

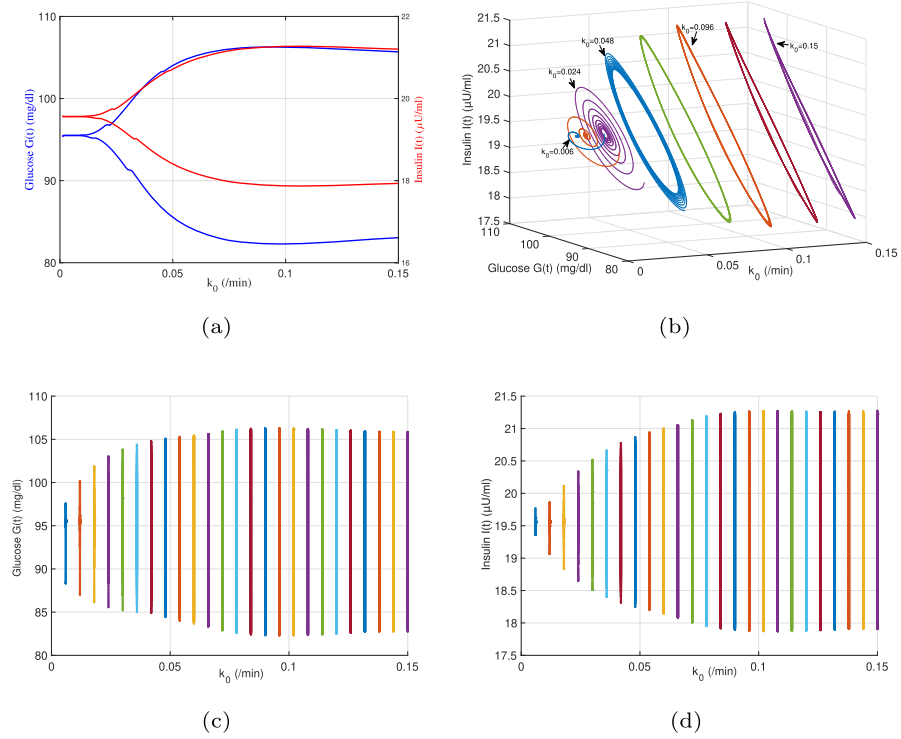


Fig. 9 **a** Hopf bifurcation diagram for the rate of insulin degradation values of k_0 , **b** the phase portrait of glucose and insulin level with values of k_0 , **c**, **d** the glucose and insulin level distributions for values of k_0 , respectively, where $\tau_1 = 20$, $\tau_2 = 60$, $G_0 = 1.35$, $d_i = 0.1$ are fixed. All other parameters are given in Table 1

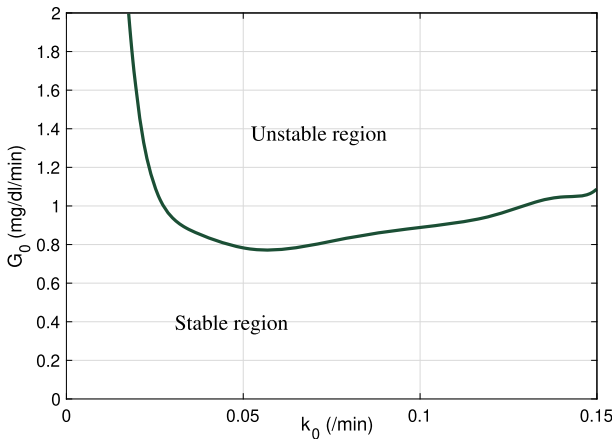


Fig. 10 Glucose infusion rate G_0 vs. insulin degradation rate k_0 while $\tau_1 = 25$, $\tau_2 = 50$, $d_i = 0.1$. The steady state of Model (2) is stable in one region and unstable in the other. All other parameters are given in Table 1

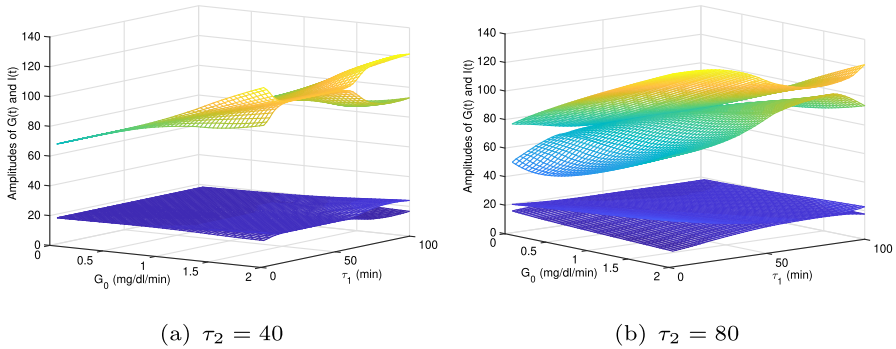


Fig. 11 Amplitudes of glucose (top) and insulin (bottom) concentrations when G_0 and τ_1 vary while **a** $\tau_2 = 40$ and **b** $\tau_2 = 80$, where $k_0 = 0.1$, $d_i = 0.1$

state of Model (2) is stable in one region and unstable in the other region. It is clear that a larger insulin degradation rate k_0 facilitates the oscillatory regulation.

4.3 Glucose infusion rate G_0 vs. τ_1 , and G_0 vs. τ_2

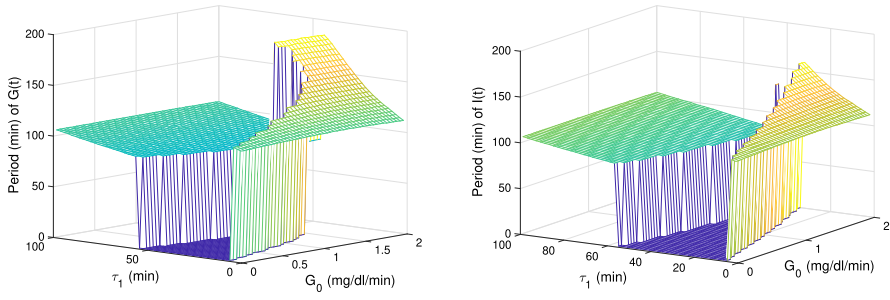
Taking the insulin response delay τ_1 and the glucose infusion rate G_0 as bifurcation parameters, we try to recognize the stability regions when $(\tau_1, G_0) \in [0, 100] \times [0, 2]$.

Let $k_0 = 0.1$, $d_i = 0.1$ be fixed and vary the value of τ_2 , the computation results are shown in Fig. 11a ($\tau_2 = 40$) and Fig. 11b ($\tau_2 = 80$). The meshes are the amplitudes of glucose (top) and insulin (bottom) concentrations for $(\tau_1, G_0) \in [0, 100] \times [0, 2]$. When $\tau_1 = 40$ (see Fig. 11a), it can be seen that two curves divide the rectangular $[0, 100] \times [0, 2]$ in the (τ_1, G_0) -plane into three regions. Increasing the value of τ_2 , the rectangular $(\tau_1, G_0) \in [0, 100] \times [0, 2]$ is divided into two regions by one curve (see Fig. 11b). The relationship between G_0 and τ_1 is nonlinear, and the sustained oscillations of Model (2) occur in the unstable regions.

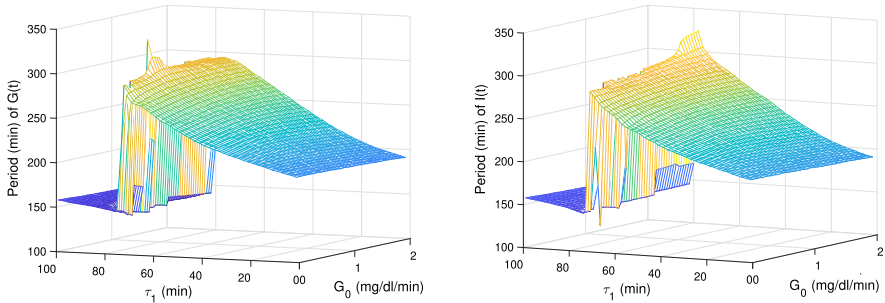
Figure 12 shows the periods of periodic solutions with different values of τ_2 , where $\tau_2 = 40$ in Fig. 12a and $\tau_2 = 80$ in Fig. 12b. Figure 13 shows the periods of periodic solutions with $\tau_1 = 20$. When $\tau_2 < 40$, the steady state is stable and no sustained oscillation will occur regardless of what value G_0 assumes where $\tau_1 = 20$ is fixed.

5 Discussion

The proposed model (2) takes a key biological factor IDE into account, which depicts the glucose-insulin regulatory slightly more comprehensive. Through the model, we qualitatively and quantitatively investigated the interaction between glucose and insulin under the impact of IDE. The existence of the Hopf bifurcations shows the systematic and intrinsic sustained oscillatory behavior of the regulatory system with various varying parameters, including the time delay τ_1 , τ_2 , the meal ingestion rate G_0 , and the natural insulin degradation rate k_0 .

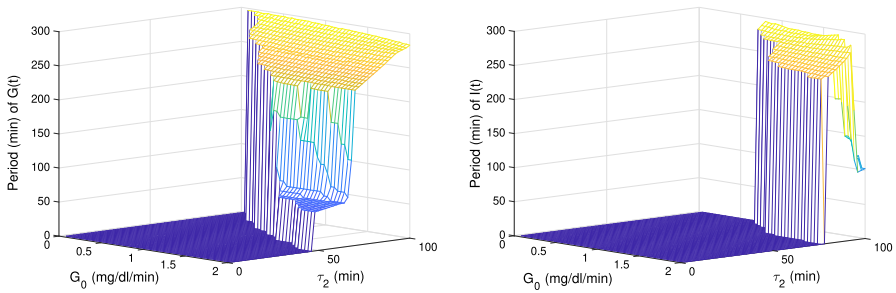


(a) $\tau_2 = 40$



(b) $\tau_2 = 80$

Fig. 12 Periods of glucose (a) and insulin (b) concentrations when G_0 and τ_1 vary while a $\tau_2 = 40$ and b $\tau_2 = 80$, where $k_0 = 0.1$, $d_i = 0.1$ are fixed



(a)

(b)

Fig. 13 Periods of glucose (left) and insulin (right) concentrations when G_0 and τ_2 vary, where $\tau_1 = 20$, $k_0 = 0.1$, $d_i = 0.1$ are fixed

By choosing time delays as the bifurcation parameters, the characteristic equation of Model (2) with two delays is investigated, and some conditions for the appearance of Hopf bifurcation that leads to the appearance of periodic solutions are obtained. We also obtain stability results for the model with two independent delays. It is worth noting that the stability of the steady state solution depends on both τ_1 and τ_2 (see Figs. 2,

4). These are the time delays that reflect the naturally occurring glucose-insulin oscillations: they reflect the finite time needed for the pancreas and the liver to secrete insulin and glucose. Glucose and insulin oscillations occur only for relatively long periods of time delay due to the instability of the stationary solution of Model (2), we observe a periodic behavior when a small time delay and chaotic behavior under long time delay in the glucose-insulin regulatory system (see Figs. 5, 6). We analytically show the existence of Hopf bifurcation when the delay parameter τ_2 increases from small, τ_1 varies in certain ranges, and k_0 increases from small, respectively (see Figs. 7, 8, 9, 10). The parameter G_0 and the delays τ_1 , τ_2 are analyzed for their influence on the glucose-insulin regulatory system. The ranges of these parameters are estimated for sustaining the oscillation of glucose and insulin, and ranges for different subjects are discussed based on simulation results (see Figs. 11, 12, 13).

In addition, simple numerical simulations (not shown) reveal that IDE deficiency (smaller c and larger \hat{I}) demonstrated the potential for abundant insulin, glucose tolerance, and possibly insulin sensitivity, while IDE overexpression (larger value of c and smaller \hat{I}) could potentially cause type 2 diabetes.

Certain limitations still exist in our proposed model (2). The time scale is relatively short to capture the slow and gradual loss of β -cell function in longitudinal dynamics observed in Costes and Butler (2014). The time delay τ_3 in the IDE impact might not be the same as the time delay τ_2 in the HGP. Also, the liver takes an important role in this metabolic system. Both HGP and IDE conduct stochastically due to the complexity of metabolism, particularly, when the pathological changes. We shall deploy these in future work.

Acknowledgements This research of F.R. is partially supported by Qing Lan Project of Jiangsu Province, NSFC (11601226), Project of Philosophy and Social Science Research in Colleges and Universities in Jiangsu Province (2021SJB0081), Postgraduate Education Reform Project of Nanjing Tech University (YJG2212), and Postgraduate Research & Practice Innovation Program of Jiangsu Province (SJCX23_0427).

Data availability Data sharing not applicable to this article as no datasets were generated or analyzed during the current study.

Declarations

Conflict of interest The authors declare that they have no conflict of interest.

Appendices

Proof of Proposition 3.1

Proof For the positive steady state solution of Model (2), we let

$$F(x) = G_0 - f_2(x) - f_3(x)f_4\left(\frac{\ln(k_0 f_1(x) + d_i)}{c}\right) + f_5\left(\frac{\ln(k_0 f_1(x) + d_i)}{c}\right) = 0, \quad x \geq 0, \quad (28)$$

and derive

$$\begin{aligned} \frac{dF(x)}{dx} = & -\frac{df_2(x)}{dx} - \frac{df_3(x)}{dx} f_4\left(\frac{\ln(k_0 f_1(x) + d_i)}{c}\right) - f_3(x) \frac{d}{dx} f_4\left(\frac{\ln(k_0 f_1(x) + d_i)}{c}\right) \\ & \cdot \frac{df_1(x)}{dx} \frac{k_0}{c(k_0 f_1(x) + d_i)} + \frac{d}{dx} f_5\left(\frac{\ln(k_0 f_1(x) + d_i)}{c}\right) \frac{df_1(x)}{dx} \frac{k_0}{c(k_0 f_1(x) + d_i)}. \end{aligned}$$

Observing that $\frac{df_i(x)}{dx} > 0$ ($i = 1, 2, 3, 4$) and $\frac{df_5(x)}{dx} < 0$, we obtain $\frac{dF(x)}{dx} < 0$. Notice that $F(0) = G_0 - f_2(0) - f_3(0) f_4\left(\frac{\ln(k_0 f_1(0) + d_i)}{c}\right) + f_5\left(\frac{\ln(k_0 f_1(0) + d_i)}{c}\right) = G_0 + f_5\left(\frac{\ln(k_0 f_1(0) + d_i)}{c}\right) > 0$, and based on the conditions (H1) – (H5), then

$$\begin{aligned} \lim_{x \rightarrow \infty} F(x) = & G_0 - \lim_{x \rightarrow \infty} f_2(x) - \lim_{x \rightarrow \infty} f_3(x) f_4\left(\frac{1}{c} \ln(\lim_{x \rightarrow \infty} k_0 f_1(x) + d_i)\right) \\ & + f_5\left(\frac{1}{c} \ln(\lim_{x \rightarrow \infty} k_0 f_1(x) + d_i)\right) \\ = & G_0 - M_2 - \lim_{x \rightarrow \infty} f_3(x) f_4\left(\frac{1}{c} \ln(k_0 M_1 + d_i)\right) + f_5\left(\frac{1}{c} \ln(k_0 M_1 + d_i)\right) \\ < & G_0 - M_2 - \lim_{x \rightarrow \infty} f_3(x) m_4 + f_5\left(\frac{1}{c} \ln(k_0 M_1 + d_i)\right) < 0. \end{aligned}$$

Due to $f_1(x)$ strictly monotone increasing, thus the proof is complete. It can be seen that G^* is the root of (28) and $I^* = \frac{1}{c} \ln(k_0 f_1(G^*) + d_i)$.

For the second part of (i), we observe that

- (a) $\left| \frac{df_i(x)}{dx} \right|, i = 1, 2, 3, 4, 5$ are bounded;
- (b) $f_i(x), i = 2, 3, 4$ and $f_j(x_t), j = 1, 5$ are Lipschitzian and completely continuous in $x \geq 0$ and $x_t \in \mathbb{C}([-\max\{\tau_1, \tau_2\}, 0])$, respectively;
- (c) $\frac{x}{e^{cx}-1} > 0, \frac{d}{dx} \left(\frac{x}{e^{cx}-1}\right) = \frac{(1-cx)e^{cx}-1}{(e^{cx}-1)^2} < 0$ and $\frac{d^2}{dx^2} \left(\frac{x}{e^{cx}-1}\right) = \frac{ce^{cx}(e^{cx}(cx-2)+cx+2)}{(e^{cx}-1)^3} > 0$ for $x > 0, \lim_{x \rightarrow 0^+} \frac{x}{e^{cx}-1} = \frac{1}{c} > 0$, then $\frac{x}{e^{cx}-1}$ is monotonically decreasing and bounded for $x > 0$;
- (d) let $\frac{x}{e^{cx}-1}|_{x=0} = \frac{1}{c}$, then $\frac{x}{e^{cx}-1}$ and $\frac{x_t}{e^{cx_t}-1}$ are respectively Lipschitzian and continuous in $x \geq 0$ and $x_t \in \mathbb{C}([-\tau_2, 0])$.

Therefore, referring to Theorems 2.1, 2.2, and 2.4 in Kuang (2012), the solution of Model (2) with the given initial condition exists and is unique for all $t \geq 0$. If there exists a $t_0 > 0$ such that $G(t_0) = 0$ and $G(t) > 0$ for $0 < t < t_0$, then $\frac{d}{dt} G(t_0) \leq 0$. But

$$\begin{aligned} \frac{d}{dt} G(t_0) = & G_0 - f_2(G(t_0)) - f_3(G(t_0)) f_4(I(t_0)) + f_5(I(t_0 - \tau_2)) \\ = & G_0 + f_5(I(t_0 - \tau_2)) > 0, \end{aligned}$$

this contradiction implies that $G(t) > 0$ for all $t > 0$. If there exists a $t'_0 > 0$ such that $I(t'_0) = 0$ and $I(t) > 0$ for all $0 < t < t'_0$, then $I(t'_0) < 0$. Notice that

$$\begin{aligned} \frac{d}{dt} I(t'_0) = & f_1(G(t'_0 - \tau_1)) \frac{k_0 I(t'_0 - \tau_2)}{e^{cI(t'_0 - \tau_2)} - 1} - k_0 I(t'_0) \\ = & f_1(G(t'_0 - \tau_1)) \frac{k_0 I(t'_0 - \tau_2)}{e^{cI(t'_0 - \tau_2)} - 1} > 0, \end{aligned}$$

this implies that $I(t) > 0$ for all $t > 0$.

Here, we prove that any given solution $(G(t), I(t))$ of Model (2) is bounded for $t > 0$. If $\limsup_{t \rightarrow \infty} G(t) = \infty$, there exists a sequence $\{t_n\}_{n=1}^\infty \uparrow \infty$ such that $\lim_{n \rightarrow \infty} G(t_n) = \infty$ and $\frac{d}{dt}G(t_n) \geq 0$. Thus $0 < \frac{d}{dt}G(t_n) = G_0 - f_2(G(t_n)) - f_3(G(t_n))f_4(I(t_n)) + f_5(I(t_n - \tau_2)) \leq G_0 - f_2(G(t_n)) - f_3(G(t_n))m_4 + M_5$, and therefore

$$\begin{aligned} \lim_{n \rightarrow \infty} \frac{d}{dt}G(t_n) &= G_0 - \lim_{n \rightarrow \infty} f_2(G(t_n)) - \lim_{n \rightarrow \infty} f_3(G(t_n))f_4(I(t_n)) \\ &\quad + \lim_{n \rightarrow \infty} f_5(I(t_n - \tau_2)) \\ &\leq G_0 - M_2 - \lim_{n \rightarrow \infty} f_3(G(t_n))m_4 + M_5 < 0. \end{aligned}$$

This contradiction shows that there is a $M_G > 0$ such that $G(t) < M_G$ for all $t > 0$. For the second equation in (2), since $|f_1(x)| \leq M_1$, for $\epsilon > 0$, $\frac{dI(t)}{dt} \leq f_1(M_G + \epsilon) \frac{k_0 I(t - \tau_2)}{e^{cI(t - \tau_2)} - 1} - k_0 I(t)$ for sufficiently large $t > 0$. If $\limsup I(t) = \infty$, there exists a sequence $\{t'_n\}_{n=1}^\infty \uparrow \infty$ such that $\lim_{n \rightarrow \infty} I(t'_n) = \infty$ and $\frac{d}{dt}I(t_n) \geq 0$. Then, $0 < \frac{d}{dt}I(t'_n) \leq f_1(M_G + \epsilon) \frac{k_0 I(t'_n - \tau_2)}{e^{cI(t'_n - \tau_2)} - 1} - d_i I(t'_n)$ and

$$\begin{aligned} \lim_{n \rightarrow \infty} \frac{d}{dt}I(t'_n) &\leq f_1(M_G + \epsilon) \lim_{n \rightarrow \infty} \frac{k_0 I(t'_n - \tau_2)}{e^{cI(t'_n - \tau_2)} - 1} - \lim_{n \rightarrow \infty} d_i I(t'_n) \\ &= 0 - \lim_{n \rightarrow \infty} d_i I(t'_n) < 0, \end{aligned}$$

this shows that there exists a $M_I > 0$ such that $I(t) < M_I$ for all $t > 0$.

If (ii) is not true, assume $\limsup_{t \rightarrow \infty} G(t) = M_G < \infty$. There exists $\{t_n\}_{n=1}^\infty \uparrow \infty$ such that $\frac{d}{dt}G(t_n) = 0$, $n = 1, 2, 3, \dots$, and $\lim_{n \rightarrow \infty} G(t_n) = M_G$ according to Lemma 3.1 (fluctuation lemma) in Li and Kuang (2007). Then $\frac{d}{dt}G(t_n) = G_0 - f_2(G(t_n)) - f_3(G(t_n))f_4(I(t_n)) + f_5(I(t_n - \tau_2)) \geq G_0 - f_2(G(t_n)) - f_3(G(t_n))m_4$. Let $n \rightarrow \infty$, thus $0 \geq G_0 - f_2(M_G) - f_3(M_G)m_4$, that is, $f_3(M_G) \geq \frac{G_0 - f_2(M_G)}{m_4}$. In addition, $f_3(M_G) \leq \lim_{x \rightarrow \infty} f_3(x) < \frac{G_0 - M_2}{m_4} \leq \frac{G_0 - f_2(M_G)}{m_4}$. \square

Proof of Lemma 3.1

Proof If $\lambda = \pm i\omega$ ($\omega > 0$) is a pair of purely imaginary roots of Eq. (9) and ω then satisfies the following equation

$$-\omega^2 + (A + B e^{-i\omega\tau_2})i\omega + D + C e^{-i\omega\tau_2} = 0. \tag{29}$$

Separating the real and imaginary parts of Eq. (29) leads to

$$\begin{cases} -\omega^2 + B\omega \sin \omega\tau_2 + C \cos \omega\tau_2 + D = 0, \\ \omega(A + B \cos \omega\tau_2) = C \sin \omega\tau_2, \end{cases} \tag{30}$$

which implies that

$$\sin \omega \tau_2 = \frac{AC\omega + B\omega(\omega^2 - D)}{C^2 + B^2\omega^2}, \quad \cos \omega \tau_2 = \frac{C(\omega^2 - D) - AB\omega^2}{C^2 + B^2\omega^2}, \quad (31)$$

and $\omega = 0$ is not a solution of (31) since $C + D > 0$. From Eq. (31), we obtain

$$\omega^4 + (A^2 - B^2 - 2D)\omega^2 + (D + C)(D - C) = 0, \quad (32)$$

then

$$\omega^2 := \omega_{\pm}^2 = \frac{-(A^2 - B^2 - 2D) \pm \sqrt{(A^2 - B^2 - 2D)^2 - 4(D + C)(D - C)}}{2}. \quad (33)$$

Clearly, if $D > C$ and $A^2 - B^2 - 2D > 0$, there are no ω such that Eq. (9) has purely imaginary roots $\pm i\omega$. If $D < C$, the number of pairs of purely imaginary roots of (9) is one. If $(A^2 - B^2 - 2D)^2 > 4(D + C)(D - C) > 0 > A^2 - B^2 - 2D$, the number of pairs of purely imaginary roots of Eq. (9) is two.

From Eq. (30), we get the following two sets of values of τ_2 for which there are imaginary roots:

$$\tau_2^{n,1} = \frac{\theta_1 + 2n\pi}{\omega_+} = \frac{1}{\omega_+} \left[\arccos \left(\frac{C(\omega_+^2 - D) - AB\omega_+^2}{C^2 + B^2\omega_+^2} \right) + 2n\pi \right], \quad n = 0, 1, \dots \quad (34)$$

where

$$\sin \theta_1 = \frac{AC\omega_+ + B\omega_+(\omega_+^2 - D)}{C^2 + B^2\omega_+^2}, \quad \cos \theta_1 = \frac{C(\omega_+^2 - D) - AB\omega_+^2}{C^2 + B^2\omega_+^2}, \quad 0 \leq \theta_1 \leq 2\pi, \quad (35)$$

and

$$\tau_2^{n,2} = \frac{\theta_2 + 2n\pi}{\omega_-} = \frac{1}{\omega_-} \left[\arccos \left(\frac{C(\omega_-^2 - D) - AB\omega_-^2}{C^2 + B^2\omega_-^2} \right) + 2n\pi \right], \quad n = 0, 1, \dots \quad (36)$$

where

$$\sin \theta_2 = \frac{AC\omega_- + B\omega_-(\omega_-^2 - D)}{C^2 + B^2\omega_-^2}, \quad \cos \theta_2 = \frac{C(\omega_-^2 - D) - AB\omega_-^2}{C^2 + B^2\omega_-^2}, \quad 0 \leq \theta_2 \leq 2\pi. \quad (37)$$

□

Proof of Lemma 3.2

Proof By differentiating Eq. (9) with respect to τ_2 , we derive

$$(2\lambda + A + (B - B\lambda\tau_2 - C\tau_2)e^{-\lambda\tau_2}) \frac{d\lambda}{d\tau_2} = (B\lambda + C)\lambda e^{-\lambda\tau_2}, \tag{38}$$

and

$$\left(\frac{d\lambda}{d\tau_2}\right)^{-1} = \frac{(2\lambda + A)e^{\lambda\tau_2} + B}{(B\lambda + C)\lambda} - \frac{\tau_2}{\lambda}, \tag{39}$$

where

$$e^{\lambda\tau_2} = -\frac{B\lambda + C}{\lambda^2 + A\lambda + D}. \tag{40}$$

Then,

$$\left(\frac{d\lambda}{d\tau_2}\right)^{-1} = -\frac{2\lambda + A}{\lambda(\lambda^2 + A\lambda + D)} + \frac{B}{(B\lambda + C)\lambda} - \frac{\tau_2}{\lambda}, \tag{41}$$

Let $\tau_2 = \tau_2^{n,k}$ ($k = 1, 2$), therefore,

$$\begin{aligned} & \text{sign} \left\{ \frac{d\text{Re}(\lambda)}{d\tau_2} \Big|_{\tau_2=\tau_2^{n,k}} \right\} \\ &= \text{sign} \left\{ \text{Re} \left(\frac{d\lambda}{d\tau_2} \right)^{-1} \Big|_{\tau_2=\tau_2^{n,k}} \right\} \\ &= \text{sign} \left\{ \text{Re} \left(-\frac{2\lambda + A}{\lambda(\lambda^2 + A\lambda + D)} \right) \Big|_{\tau_2=\tau_2^{n,k}} + \text{Re} \left(\frac{B}{(B\lambda + C)\lambda} \right) \Big|_{\tau_2=\tau_2^{n,k}} \right\} \\ &= \text{sign} \left\{ \frac{A^2 - 2(D - \omega_{k,n}^2)}{(D - \omega_{k,n}^2)^2 + A^2\omega_{k,n}^2} - \frac{B^2}{C^2 + B^2\omega_{k,n}^2} \right\} \\ &= \text{sign} \{ A^2 - B^2 - 2D + 2\omega_{k,n}^2 \}. \end{aligned} \tag{42}$$

By inserting the expression for $\omega_{k,n}^2$ ($k = 1, 2$), it is seen that $\text{sign}\{A^2 - B^2 - 2D + 2\omega_{k,n}^2\} > 0$ for $\tau_2^{n,1}$ and ω_+^2 ; and $\text{sign}\{A^2 - B^2 - 2D + 2\omega_{k,n}^2\} < 0$ for $\tau_2^{n,2}$ and ω_-^2 . □

Proof of Theorem 3.1

Proof Based on the above Lemmas 3.1 and 3.2, we note that if $D < C$, a pair of purely imaginary roots exists $\lambda(\tau_2)|_{\tau_2=\tau_2^{n,1}} = \pm i\omega_+$ ($n = 0, 1, \dots$), then the only crossing

of the imaginary axis is from left to right as $\tau_2^{n,1}$ increases, and the stability of the steady state solution can only be lost and not regained. If $A^2 - B^2 - 2D < 0$ and $(A^2 - B^2 - 2D)^2 > 4(D + C)(D - C) > 0$, crossing from left to right with increasing $\tau_2^{n,1}$ occurs whenever $\tau_2^{n,1}$ assumes a value corresponding to ω_+ , and crossing from right to left occurs for values of $\tau_2^{n,2}$ corresponding to ω_- .

In the case that $D < C$, only $\tau_2^{0,1}$ need be considered, since if Model (2) is asymptotically stable for $\tau_2 = 0$, then it remains asymptotically stable until $\tau_2^{0,1}$, and it is unstable thereafter. At $\tau_2 = \tau_2^{0,1}$, Eq. (9) has pure imaginary roots $\pm i\omega_+$.

In the case of $(A^2 - B^2 - 2D)^2 > 4(D + C)(D - C) > 0 > A^2 - B^2 - 2D$, if Model (2) is stable for $\tau_2 = 0$, then it must follow that $\tau_2^{0,1} < \tau_2^{0,2}$ since the multiplicity of roots with positive real parts cannot become negative. We observe that

$$\tau_2^{n+1,1} - \tau_2^{n,1} = \frac{2\pi}{\omega_+} < \frac{2\pi}{\omega_-} = \tau_2^{n+1,2} - \tau_2^{n,2}, \tag{43}$$

with $\omega_+ > \omega_- > 0$. Thus, there can be only a finite number of switches between stability and instability. Moreover, there exist values of the parameters that realize any number of such stability switches. However, there exists a $\hat{\tau}_2$ such that at $\tau_2 = \hat{\tau}_2$ a stability switch occurs from stable to unstable, and for $\tau_2 > \hat{\tau}_2$ the solution remains unstable. If Model (2) is unstable for $\tau_2 = 0$, then a similar argument as before can be made. Model (2) can either be unstable for $\tau_2 > 0$ or exhibit any number of stability switches as in the preceding case.

As τ_2 is increased, the multiplicity of roots for which $\text{Re}(\lambda) > 0$ is increased by two whenever τ_2 passes through a value of $\tau_2^{n,1}$ and it is decreased by two whenever τ_2 passes through a value of $\tau_2^{n,2}$.

When the steady state solution is stable for $\tau_2 = 0$, j switches from stability to instability to stability occur when the parameters are such that

$$\tau_2^{0,1} < \tau_2^{0,2} < \tau_2^{1,1} < \dots < \tau_2^{j-1,1} < \tau_2^{j-1,2} < \tau_2^{j,1} < \tau_2^{j+1,1} < \tau_2^{j,2} \dots ,$$

or j switches from instability to stability to instability may occur when

$$\tau_2^{0,2} < \tau_2^{0,1} < \tau_2^{1,2} < \dots < \tau_2^{j-1,2} < \tau_2^{j-1,1} < \tau_2^{j,1} < \tau_2^{j,2} \dots ,$$

when the steady state solution is stable for $\tau_2 = 0$. The conditions on the parameters in order that the preceding orderings be valid can be formulated directly from Eqs. (34)-(37).

From the above analysis, we obtain the theorem results. □

Proof of Theorem 3.3

Proof Let $\lambda = \alpha + i\omega_0$ ($\alpha \in \mathbb{R}$, $\omega_0 = 2q\pi > 0$) be a root of Eq. (5), then for $\mathbf{g}(\lambda) = W_5 e^{-\lambda\tau_2} \lambda + W_2 W_4 e^{-\lambda\tau_1} + W_1 W_5 e^{-\lambda\tau_2} + W_3 W_4 e^{-\lambda(\tau_1+\tau_2)} = 0$ we have

$$\begin{cases} \operatorname{Re}(\mathbf{g}(\lambda)) = W_5 e^{-\alpha\tau_2} (\alpha \cos \omega_0 \tau_2 + \omega_0 \sin \omega_0 \tau_2) + W_2 W_4 e^{-\alpha\tau_1} \cos \omega_0 \tau_1 \\ \quad + W_1 W_5 e^{-\alpha\tau_2} \cos \omega_0 \tau_2 + W_3 W_4 e^{-\alpha(\tau_1+\tau_2)} \cos \omega_0 (\tau_1 + \tau_2) = 0, \\ \operatorname{Im}(\mathbf{g}(\lambda)) = W_5 e^{-\alpha\tau_2} (\omega_0 \cos \omega_0 \tau_2 - \alpha \sin \omega_0 \tau_2) - W_2 W_4 e^{-\alpha\tau_1} \sin \omega_0 \tau_1 \\ \quad - W_1 W_5 e^{-\alpha\tau_2} \sin \omega_0 \tau_2 - W_3 W_4 e^{-\alpha(\tau_1+\tau_2)} \sin \omega_0 (\tau_1 + \tau_2) = 0. \end{cases} \quad (44)$$

In order to simplify, let us consider $q\tau_2 \in \mathbb{Z}^+$, Eq. (44) has the following form

$$\begin{cases} \operatorname{Re}(\mathbf{g}(\lambda)) = (\alpha W_5 + W_1 W_5) e^{-\alpha\tau_2} + (W_2 W_4 e^{-\alpha\tau_1} + W_3 W_4 e^{-\alpha(\tau_1+\tau_2)}) \cos \omega_0 \tau_1 = 0, \\ \operatorname{Im}(\mathbf{g}(\lambda)) = \omega_0 W_5 e^{-\alpha\tau_2} - (W_2 W_4 e^{-\alpha\tau_1} + W_3 W_4 e^{-\alpha(\tau_1+\tau_2)}) \sin \omega_0 \tau_1 = 0, \end{cases} \quad (45)$$

we can obtain

$$\begin{cases} \tan(\omega_0 \tau_1) = -\frac{\omega_0}{\alpha + W_1}, \\ (W_2 W_4 e^{-\alpha\tau_1} + W_3 W_4 e^{-\alpha(\tau_1+\tau_2)})^2 = (\omega_0^2 + (\alpha + W_1)^2) W_5^2 e^{-2\alpha\tau_2}. \end{cases} \quad (46)$$

If there exists a constant $\alpha_0 < 0$ satisfies (46), then $\mathbf{g}(\lambda)$ has at least one zero $\lambda_0 = \alpha_0 + i\omega_0$ with $\alpha_0 < 0$.

Let

$$X(\alpha) = (W_2 W_4 e^{-\alpha\tau_1} + W_3 W_4 e^{-\alpha(\tau_1+\tau_2)})^2 - (\omega_0^2 + (\alpha + W_1)^2) W_5^2 e^{-2\alpha\tau_2}. \quad (47)$$

Notice that $X(0) = (W_2 W_4 + W_3 W_4)^2 - \omega_0^2 W_5^2 - W_1^2 W_5^2 < 0$ if $W_2 W_4 + W_3 W_4 \leq W_1 W_5$ and $\lim_{\alpha \rightarrow -\infty} X(\alpha) = +\infty$. Furthermore, taking $\alpha = -W_1$, then

$$\begin{aligned} X(-W_1) &= (W_2 W_4 e^{W_1\tau_1} + W_3 W_4 e^{W_1(\tau_1+\tau_2)})^2 - \omega_0^2 W_5^2 e^{2W_1\tau_2} \\ &> (W_2 W_4 e^{W_1\tau_1} + W_3 W_4 e^{W_1\tau_1})^2 - \omega_0^2 W_5^2 e^{2W_1\tau_2}. \end{aligned} \quad (48)$$

If $\tau_2 - \tau_1 \leq T_0 = \frac{1}{W_1} \ln \frac{W_2 W_4 + W_3 W_4}{\omega_0 W_5}$ such that $X(-W_1) \geq 0$, then there is a constant $\alpha_0 \in (-W_1, 0)$ satisfies $X(\alpha_0) = 0$. Thus, $\lambda_0 = \alpha_0 + i\omega_0$ is the zero point of $\mathbf{g}(\lambda)$.

In the following, we construct a simple loop L homotopic to a point and then show $|\mathbf{g}(\lambda)| > |\mathbf{f}(\lambda)|$ on L . We divide the simple loop L into two parts as: one is defined by taking $(-W_1, 0)$ and $\sqrt{W_1^2 + \omega_0^2}$ as a center point and the radius, respectively; the other is defined as $\lambda = i\omega$, $\omega \in [-\omega_0, \omega_0]$.

Let $\lambda = x + i\omega$ with $x \in [-W_1 - \sqrt{W_1^2 + \omega_0^2}, 0]$ and $\omega \in [-\omega_0, \omega_0]$, we set $x = b\alpha_0$ ($b > 0$) and then deduce

$$|\mathbf{g}(\lambda)| = |x W_5 e^{-x\tau_2} e^{-i\omega\tau_2} + i\omega W_5 e^{-x\tau_2} e^{-i\omega\tau_2} + W_2 W_4 e^{-x\tau_1} e^{-i\omega\tau_1}$$

$$\begin{aligned}
 & + W_1 W_5 e^{-x\tau_2} e^{-i\omega\tau_2} + W_3 W_4 e^{-x(\tau_1+\tau_2)} e^{-i\omega(\tau_1+\tau_2)} | \\
 = & |x W_5 e^{-x\tau_2} \cos \omega\tau_2 + \omega W_5 e^{-x\tau_2} \sin \omega\tau_2 + W_2 W_4 e^{-x\tau_1} \cos \omega\tau_1 \\
 & + W_1 W_5 e^{-x\tau_2} \cos \omega\tau_2 + W_3 W_4 e^{-x(\tau_1+\tau_2)} \cos \omega(\tau_1 + \tau_2) \\
 & + i(\omega W_5 e^{-x\tau_2} \cos \omega\tau_2 - x W_5 e^{-x\tau_2} \sin \omega\tau_2 - W_2 W_4 e^{-x\tau_1} \sin \omega\tau_1 \\
 & - W_1 W_5 e^{-x\tau_2} \cos \omega\tau_2 - W_3 W_4 e^{-x(\tau_1+\tau_2)} \sin \omega(\tau_1 + \tau_2)) | \\
 > & W_1 W_5 e^{-b\alpha_0\tau_2} + W_2 W_4 e^{-b\alpha_0\tau_1} - W_3 W_4 e^{-b\alpha_0(\tau_1+\tau_2)} > \frac{W_1 W_5 + W_2 W_4}{2}.
 \end{aligned} \tag{49}$$

Let $\lambda = i\omega$, $\omega \in [-\omega_0, \omega_0]$, then

$$\begin{aligned}
 |\mathbf{g}(\lambda)| & = |W_5 e^{-i\omega\tau_2} i\omega + W_2 W_4 e^{-i\omega\tau_1} + W_1 W_5 e^{-i\omega\tau_2} + W_3 W_4 e^{-i\omega(\tau_1+\tau_2)}| \\
 & \geq W_1 W_5 + W_2 W_4 - W_3 W_4 := \eta_1 > 0.
 \end{aligned} \tag{50}$$

Let $\eta = \min \left\{ \frac{W_1 W_5 + W_2 W_4}{2}, \eta_1 \right\}$. Denote

$$\begin{aligned}
 L := & \left\{ \lambda = x + i\omega \in \mathbb{C} : \right. \\
 & (x + W_1)^2 + \omega^2 = W_1^2 + \omega_0^2, x \in [-W_1 - \sqrt{W_1^2 + \omega_0^2}, 0], \\
 & \left. \text{or } \lambda = i\omega, \omega \in [-\omega_0, \omega_0] \right\}.
 \end{aligned} \tag{51}$$

where \mathbb{C} is a connected region. It is known that L is a simple loop homotopic to the original, $\lambda_0 = \alpha_0 + i\omega_0 \in L$ and $|\mathbf{g}(\lambda)| > \eta$ on L . Taking $r_0 > 0$ such that $L \subset \Omega := \{\lambda \in \mathbb{C} : |\lambda| < r_0\}$. Denote $\partial\Omega := \{\lambda \in \mathbb{C} : |\lambda| = r_0\}$, then for all $\lambda \in \partial\Omega$, $\lambda = r_0 e^{i\phi}$, $\phi \in [\frac{\pi}{2}, \frac{3\pi}{2}]$, we obtain

$$|\mathbf{f}(\lambda)| = |\lambda^2 + (W_1 + d_i)\lambda + W_1 d_i| \leq r_0^2 + (W_1 + d_i)r_0 + W_1 d_i. \tag{52}$$

If $r_0^2 + (W_1 + d_i)r_0 + W_1 d_i < \eta$, then for all $\lambda \in \Omega$, $\lambda = r e^{i\phi}$ and $r < r_0$, we have $|\mathbf{f}(\lambda)| < r_0^2 + (W_1 + d_i)r_0 + W_1 d_i < \eta$ for $\lambda \in L$. Therefore $|\mathbf{g}(\lambda)| > |\mathbf{f}(\lambda)|$ on L . By Rouchè's theorem, $\mathbf{g}(\lambda)$ and $\mathbf{g}(\lambda) + \mathbf{f}(\lambda)$ have the same number of zero in L . That is, $\mathbf{g}(\lambda) + \mathbf{f}(\lambda) = 0$ has at least one root $\lambda^* \in L$. □

Proof of Lemma 3.4

Proof Suppose that Eq. (9) has no root with nonnegative real parts for $\tau_2 > 0$, which means the characteristic Eq. (26) with $\tau_1 = 0$ and $\tau_2 > 0$ has no root with a nonnegative real part.

Using τ_1 as a variable, then the left-hand side of Eq. (26) is analytic in λ and τ_1 , and the sum of the multiplicities of zeros of the left-hand side of Eq. (26) in the open right half-plane can only change if a zero appears on or crosses the imaginary axis.

Due to Eq. (26) with $\tau_1 = 0$ has no root with nonnegative real part, there is $\tau_1^*(\tau_2) > 0$ such that all roots of Eq. (26) have negative real parts when $0 < \tau_1 < \tau_1^*(\tau_2)$. □

References

- Abdul-Hay SO, Kang D, McBride M, Li L, Zhao J, Leissring MA (2011a) Deletion of insulin-degrading enzyme elicits antipodal, age-dependent effects on glucose and insulin tolerance. *PLoS ONE* 6(6):e20818
- Batzel J, Kappel F (2011) Time delay in physiological systems: analyzing and modeling its impact. *Math Biosci* 234(2):61–74
- Beretta E, Kuang Y (2002) Geometric stability switch criteria in delay differential systems with delay dependent parameters. *SIAM J Math Anal* 33(5):1144–1165
- Bergman R, Ider Y, Bowden C, Cobelli C (1979) Quantitative estimation of insulin sensitivity. *Am J Physiol* 236(6):667–677
- Bolie V (1961) Coefficients of normal blood glucose regulation. *J Appl Physiol* 16(5):783–788
- Broh-Kahn R, Mirsky I (1949) The inactivation of insulin by tissue extracts; the effect of fasting on the insulinase content of rat liver. *Arch Biochem* 20(1):10–4
- Chen C, Tsai H (2010) Modeling the physiological glucose-insulin system on normal and diabetic subjects. *Comput Methods Programs Biomed* 97(2):130–40
- Cooke K, Grossman Z (1982) Discrete delay, distributed delay and stability switches. *J Math Anal Appl* 86:592–627
- Costes S, Butler PC (2014) Insulin-degrading enzyme inhibition, a novel therapy for type 2 diabetes? *Cell Metab* 20(2):201–203
- Engelborghs K, Lemaire V, Bélair J, Roose D (2001) Numerical bifurcation analysis of delay differential equations arising from physiological modeling. *J Math Biol* 42(4):361–385
- Farris W, Mansourian S, Chang Y, Lindsley L, Eckman E, Frosch M, Eckman C, Tanzi R, Selkoe D, Guénette S (2003) Insulin-degrading enzyme regulates the levels of insulin, amyloid β -protein, and the β -amyloid precursor protein intracellular domain in vivo. *Proc Natl Acad Sci USA* 100(7):4162–4167
- Fawcett J, Duckworth W (2009) Hyperglycaemia and hyperinsulinaemia: is insulin-degrading enzyme the missing link. *Diabetologia* 52:1457–1460
- Fernández-Díaz CM, Merino B, López-Acosta JF, Ciudad P, de la Fuente MA, Lobatón CD, Moreno A, Leissring MA, Perdomo G, Cózar-Castellano I (2019) Pancreatic β -cell-specific deletion of insulin-degrading enzyme leads to dysregulated insulin secretion and β -cell functional immaturity. *Am J Physiol Endocrinol Metab* 317(5):E805–E819
- Galagovsky D, Katz M, Acevedo J, Soriano E, Glavic A, Wappner P (2014) The *Drosophila* insulin-degrading enzyme restricts growth by modulating the PI3K pathway in a cell-autonomous manner. *Mol Biol Cell* 25(6):916–924
- González-Casimiro C, Merino B, Casanueva-Álvarez E, Postigo-Casado T, Cámara-Torres P, Fernández-Díaz C, Leissring M, Cózar-Castellano I, Perdomo G (2021) Modulation of insulin sensitivity by insulin-degrading enzyme. *Biomedicine* 9(1):86
- Gu H, Efendic S, Nordman S, Ostenson C, Brismar K, Brookes A, Quantitative J (2004) Quantitative trait loci near the insulin-degrading enzyme (IDE) gene contribute to variation in plasma insulin levels. *Diabetes* 53(8):2137–42
- Huang M, Li J, Song X, Guo H (2012) Modeling impulsive injections of insulin: towards artificial pancreas. *SIAM J Appl Math* 72(5):1524–1548
- Huard B, Easton J, Angelova M (2015) Investigation of stability in a two-delay model of the ultradian oscillations in glucose-insulin regulation. *Commun Nonlinear Sci Numer Simul* 26(1–3):211–222
- IDF, International diabetes federation: diabetes facts & figures. <https://www.idf.org>. 03 Feb 2020
- Keener J, Sneyd J (2009) *Mathematical physiology*. Springer, Berlin
- Kissler SL, Cichowitz C, Sankaranarayanan S, Bortz D (2014) Determination of personalized diabetes treatment plans using a two-delay model. *J Theor Biol* 359:101–111
- Kuang Y (2012) *Delay differential equations: with applications in population dynamics*. Academic Press, Boston
- Kukday SS, Manandhar SP, Ludley MC, Burriss ME, Alper BJ, Schmidt WK (2012) Cell-permeable, small-molecule activators of the insulin-degrading enzyme. *J Biomol Screen* 17(10):1348–1361
- Kuo W, Gehm B, Rosner M, Li W, Keller G (1994) Inducible expression and cellular localization of insulin-degrading enzyme in a stably transfected cell line. *J Biol Chem* 269(36):22599–606
- Li J, Kuang Y (2007) Analysis of a model of the glucose-insulin regulatory system with two delays. *SIAM J Appl Math* 67(3):757–776

- Li J, Kuang Y, Mason C (2006) Modeling the glucose-insulin regulatory system and ultradian insulin secretory oscillations with two explicit time delays. *J Theor Biol* 242(3):722–35
- Maianti J, McFedries A, Foda Z, Kleiner R, Du X, Leissring M, Tang W, Charron M, Seeliger M, Saghatelian A, Liu D (2014) Anti-diabetic activity of insulin-degrading enzyme inhibitors mediated by multiple hormones. *Nature* 511:84–98
- Malito E, Hulse R, Tang W (2008) Amyloid β -degrading cryptidases: insulin degrading enzyme, neprilysin, and presequence peptidase. *Cell Mol Life Sci* 65(16):2574–2585
- Merino B, Fernández-Díaz CM, Parrado-Fernández C, González-Casimiro CM, Postigo-Casado T, Lobatón CD, Leissring MA, Cózar-Castellano I, Perdomo G (2020) Hepatic insulin-degrading enzyme regulates glucose and insulin homeostasis in diet-induced obese mice. *Metabolism* 113:154352
- Mirsky I, Perisutti G, Diengott D (1955) Effect of insulinase-inhibitor on destruction of insulin by intact mouse. *Proc Soc Exp Biol Med* 88(1):76–78
- Nguyen B, Ho Y, Wu Z, Chui C (2012) Implementation of model predictive control with modified minimal model on low-power RISC microcontrollers. In: *Proceedings of the third symposium on information and communication technology*, pp 165–171
- Pei L, Wang Q, Shi H (2011) Bifurcation dynamics of the modified physiological model of artificial pancreas with insulin secretion delay. *Nonlinear Dyn* 63:417–427
- Pivovarova-Ramich O, Höhn A, Grune T, Pfeiffer A, Rudovich N (2016) Insulin-degrading enzyme: new therapeutic target for diabetes and alzheimer's disease? *Ann Med* 48(8):1–11
- Ruan S, Wei J (2003) On the zeros of transcendental functions with applications to stability of delay differential equations with two delays. *Dyn Contin Discrete Impuls Syst* 10:863–874
- Sarika W, Lenbury Y, Kumnungkit K, Kunphasuruang W (2008) Modelling glucose-insulin feedback signal interchanges involving β -cells with delays. *Sci Asia* 34(1):077–086
- Shen Y, Joachimiak A, Rosner M, Tang W (2006) Structures of human insulin-degrading enzyme reveal a new substrate recognition mechanism. *Nature* 443:870–874
- Song X, Huang M, Li J (2014) Modeling impulsive insulin delivery in insulin pump with time delays. *SIAM J Appl Math* 74(6):1763–1785
- Strilka R, Armen S, Indeck M (2014) Qualitative analysis of subcutaneous Lispro and regular insulin injections for stress hyperglycemia: a pilot numerical study. *J Theor Biol* 356:192–200
- Strilka R, Stull M, Clemens M, McCaver S, Armen S (2016) Simulation and qualitative analysis of glucose variability, mean glucose, and hypoglycemia after subcutaneous insulin therapy for stress hyperglycemia. *Theor Biol Med Model* 13(1):3
- Stull M, Strilka R, Clemens M, Armen S (2016) Comparison of subcutaneous regular insulin and lispro insulin in diabetics receiving continuous nutrition: a numerical study. *J Diabetes Sci Technol* 10(1):137–144
- Sturis J, Polonsky K, Mosekilde E, Cauter E (1991) Computer model for mechanisms underlying ultradian oscillations of insulin and glucose. *Am J Physiol* 260(5):E801–9
- Tandl E, Kolb H (1984) Insulin degrading enzyme activity and insulin binding of erythrocytes in normal subjects and type 2 (non-insulin-dependent) diabetic patients. *Diabetologia* 27(1):17–22
- Tolic I, Mosekilde E, Sturis J (2000) Modeling the insulin-glucose feedback system: the significance of pulsatile insulin secretion. *J Theor Biol* 207(3):361–75
- Torres N, Santos G (2015) The (mathematical) modeling process in biosciences. *Front Genet* 6:354
- Tsuda M, Kobayashi T, Matsuo T, Aigaki T (2010) Insulin-degrading enzyme antagonizes insulin-dependent tissue growth and Abeta-induced neurotoxicity in *Drosophila*. *FEBS Lett* 584(13):2916–2920
- Tundo G, Sbardella D, Ciaccio C, Grasso G, Gioia M, Coletta A, Polticelli F, Piero D, Milardi D, Endert P, Marini S, Coletta M (2017) Multiple functions of insulin-degrading enzyme: a metabolic crosslight? *Crit Rev Biochem Mol Biol* 52(5):554–582
- Wang H, Li J, Kuang Y (2007) Mathematical modeling and qualitative analysis of insulin therapies. *Math Biosci* 210(1):17–33
- Wei J, Ruan S (1999) Stability and bifurcation in a neural network model with two delays. *Physica D* 130:255–272
- Wu Z, Chui C, Hong G, Chang S (2011) Physiological analysis on oscillatory behavior of glucose-insulin regulation by model with delays. *J Theor Biol* 280(1):1–9
- Wu Z, Chui C, Hong G, Khoo E, Chang S (2013) Glucose-insulin regulation model with subcutaneous insulin injection and evaluation using diabetic inpatients data. *Comput Methods Programs Biomed* 111(2):347–356

Publisher's Note Springer Nature remains neutral with regard to jurisdictional claims in published maps and institutional affiliations.

Springer Nature or its licensor (e.g. a society or other partner) holds exclusive rights to this article under a publishing agreement with the author(s) or other rightsholder(s); author self-archiving of the accepted manuscript version of this article is solely governed by the terms of such publishing agreement and applicable law.